TÉCNICO LISBOA

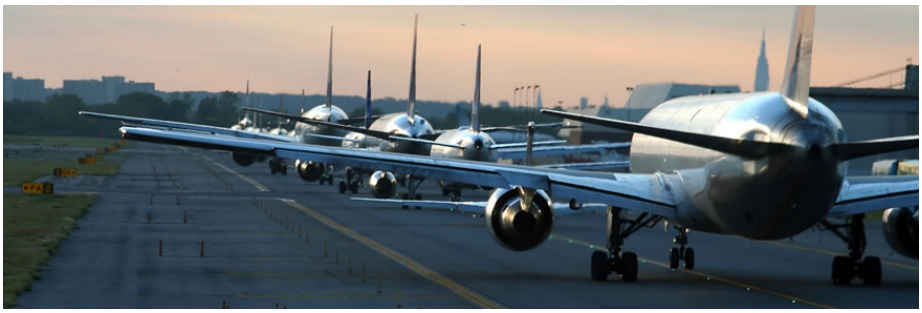

Operationalization of an AMAN system: arrival procedures adherence study

Teresa Margarida Dantas dos Reis

Thesis to obtain the Master of Science Degree in

Aerospace Engineering

Supervisors: Prof. Rodrigo Martins de Matos Ventura
Eng. José dos Santos Mestre Vermelhudo
Eng. Paulo Adelino Antunes Monteiro

Examination Committee

Chairperson: Prof. João Manuel Lage de Miranda Lemos
Supervisor: Prof. Rodrigo Martins de Matos Ventura
Member of the Committee: Prof. Pedro da Graça Tavares Alvares Serrão

November 2015

”Neste espaço a si próprio condenado
Dum momento para o outro pode entrar
Um pássaro que levante o céu
E sustente o olhar”

Alexandre O’Neill

Acknowledgments

This thesis was developed under a protocol established between NAV Portugal and Instituto Superior Técnico.

I would like to thank the staff at the DEP/ATM department at NAV for welcoming both my colleague Duarte and I, into their installations with sympathy and always willing to help. Particularly José Vermelhudo for sheltering this work, Paulo Monteiro for all his guidance, dedication and coordination throughout it and Miguel Seabra and Paulo Ceia for the support and friendship. Our room was definitely the most fun.

I also have to thank professor Rodrigo Ventura at IST for making this internship possible and choosing me as the intern. I hope he is as proud of this work as I am. Bits of it were thrived by his ideas and input and for that I am also grateful.

I would like to thank my friends, because I can not imagine not having them. Thank you for being my confidents and counselors, my inspiration at times, my daily companions, my adventure's companions when I needed to escape, my joy, my lovers, my friends.

Lastly but most importantly, I would like to thank my family for being awesome. My mother for being the most loving and devoted person I know and that knows me the best. For believing in me more than I ever do. My father for always letting me go but always being there to pick me up. For being my biggest inspiration to work hard, part of it because I would never want to disappoint him. Both of them for loving me unconditionally and making me want to be the best person I can be every day.

Resumo

Qualquer voo RNAV tem um plano de voo no qual lhe vem atribuída uma rota pré concebida para aproximação à pista e aterragem. Essa rota é chamada STAR e é definida por um conjunto de pontos fixos que a aeronave deve seguir. A TMA de um aeroporto é composta por um conjunto de STARs que garantem a total expedição de tráfego.

Esta tese foi desenvolvida no âmbito de um protocolo estabelecido entre a NAV Portugal e o Instituto Superior Técnico. Estuda o comportamento verdadeiro das aeronave na estrutura do espaço aéreo da TMA. Em última análise, visa auxiliar no redesenho deste setor, a fim de melhor integrar o AMAN no sistema.

Foram fornecidos três meses de dados SDPS e FDPS da FIR de Lisboa. Um conjunto de programas foi criado para analisar estatisticamente os dados e três análises principais foram feitas: Adherence, Average STARs e Point Direct.

A Adherence testa a taxa de adesão das aeronaves à STAR que lhes vem atribuída. Dos dados de radar extraímos a trajetória real e dos dados de plano de voo a STAR. A Adherence é um teste ao seguimento da rota pela trajetória real. Pode ser realizada em 2D ou 3D.

Average STARs extrai padrões de dados reais. Considerando as trajetórias que não estão em conformidade com a STAR, foram traçadas rotas alternativas fim de melhor se representar o comportamento real. Para cada STAR foram traçadas três rotas alternativas, sendo que cada rota segue um algoritmo diferente. O primeiro algoritmo corresponde à média, o segundo é uma média ponderada iterativa e, por último, a mediana. Considerando a trajetória como sendo um conjunto de pontos, a média calcula o ponto médio, ponto por ponto. A méda ponderada iterativa corrige a rota Média iterativamente: os pontos mais próximos ao ponto médio têm um peso maior sobre os cálculos e os mais distantes pesam menos. Por último, a mediana calcula a mediana, ponto por ponto.

Muitas vezes verificou-se que os pilotos foram instruídos ou concedidos voos directos até um determinado ponto da STAR, já dentro da TMA. Point Direct estuda a quantidade de voos directos concedidos e que pontos da STAR tiveram maior incidência.

Palavras-chave: AMAN, STAR, TMA, Desenho do Espaço Aéreo, Análise Estatística

Abstract

Every RNAV flight has a flight plan that includes a pre planned route for approaching the airport for landing. This route is called a STAR and is defined by a set of fixed points for the aircraft to follow. The TMA structure of an airport contains a set of STARs that ensure incoming traffic's expedition.

This thesis was developed under a protocol established between NAV Portugal and Instituto Superior Técnico. It studies aircraft's real behaviour in the TMA's airspace structure. Ultimately it aims to assist on the redesign of this sector in order to best integrate AMAN into the system.

Three months of SDPS and FDPS data from Lisbon's FIR were provided. A set of programs was created to statistically analyse the data and three main analysis were made: Adherence, Average STARs and Point Direct.

Adherence tests aircraft's adherence rate to its STAR. Taking the real trajectory from radar data and the assigned STAR from flight plan data, Adherence is a test on how well this route is followed. It is available in 2D and 3D.

Average STARs extracts patterns from real data. Taking trajectories that did not conform to the STAR, alternative routes were traced in order to best represent the real behaviour. For each STAR, three routes were traced. Each route followed a different algorithm. The first one being the Average, then the iterative Weighted Average and lastly the Median. Considering a track as a set of points, the Average calculates the average point, point by point. The iterative Weighted Average corrects the Average route iteratively: the points closest to the average point have a higher weight on the calculations and the furthest ones weigh less. Lastly, the Median calculates the median point, point by point.

Often was found that pilots were granted direct flights to a STAR point inside the TMA, instead of following the route from the start. Point Direct studies how many direct flights were granted and which STAR points had higher incidences.

Keywords: AMAN, STAR, TMA, Airspace Design, Statistical Analysis

Contents

List of Tables

List of Figures

Glossary

ACC	Air Traffic Control Center or Area Control Centre.
AMAN	Arrival Manager.
ANSP	Air Navigation Service Provider.
ATCO	Air Traffic Controller.
ATC	Air Traffic Control.
ATM	Air Traffic Management.
ATS	Air Traffic Services.
DEP/ATM	Directorate of Studies and Projects for Air Traffic Management.
EEC	Eurocontrol Experimental Center.
ETA	Estimated Time of Arrival.
EUROCONTROL	European Organisation for the Safety of Air Navigation.
FDPS	Flight Data Processing System.
FIR	Flight Information Region.
FP	Flight Plan.
HMI	Human-Machine Interface.
IFR	Instrument Flight Rules.
ILS	Instrument Landing System.
IST	Instituto Superior Técnico.
LAX	Los Angeles International Airport.
LISATM	Air Traffic Management System on Lisbon's Flight Information Region.
LPPR	ICAO code for Francisco Sá Carneiro Airport in Oporto.
LPPT	ICAO code for Portela Airport in Lisbon.
LSSIP	Local Single Sky Implementation.
MTF	Medium-Term Forecast.
NATS UK	UK Air Navigation Service Provider.

NAV Portugal	Portugal Air Navigation Service Provider.
OSYRIS	Barco's Air Traffic Management software: Queue Management.
PM	Point Merge.
QGIS	Quantum Geographic Information System.
QNH	Q code for the barometric pressure adjusted to sea level.
RFM	Relative File Management.
RNAV	Area Navigation.
RWY	Runway.
SDPS	Surveillance Data Processing System.
SESAR	Single European Sky ATM Research.
SES	Single European Sky.
SID	Standard Instrument Departure Route.
STAR	Standard Arrival Route.
STA	Scheduled Time of Arrival.
STRATFOR	Stratfor is a geopolitical intelligence firm that provides strategic analysis and forecasting to individuals and organizations around the world.
TCA	Terminal Control Approach.
TMA	Terminal Maneuvering Area.
TOD	Time Of Day.
iTEC	interoperability Through European Collaboration.

Chapter 1

Introduction

Arrival Management systems are controllers support tools. They are intended to help air traffic controllers to efficiently manage incoming flights in order to make best use of available runway and airspace capacities. Specifically, the AMAN systems provide an aircraft sequence and an expected or scheduled time for each flight at the runway or at/over different fixes.

Since the late 1990s, AMAN systems have been developed all accross Europe without a centralized or standardized approach. In Portugal, a system with the name OSYRIS was bought in 2010. Its HMI is planned to be developed and fine-tuned locally by NAV Portugal. According to the LSSIP document for Portugal 2014 [1], both the AMAN tools implementation as well as the AMAN/OSYRIS integration into LISATM are expected by the end of 2018.

1.1 Motivation

"Traffic in Portugal increased by 7.5% during summer 2014 (May to October), when compared to the same period of 2013. The STRATFOR medium-term forecast (MTF) predicts an average annual increase of between 0.8% and 4.2%, with a baseline growth of 2.5% for the Lisbon FIR during the planning cycle. The average en route delay per flight increased from 0.2 minutes per flight in summer 2013 to 0.29 minutes per flight in summer 2014. 63% of the delays were caused by ATC Capacity and 33% for ATC Staffing". [1] From January until June of 2015, traffic in Lisbon FIR has increased by 4.3%, when compared to the same period of 2014. This data is graphically shown in Figure 1.1.

AMAN will increase airport capacity by assisting air traffic controllers on managing incoming flights and therefore reducing controller workload. The OSYRIS system in particular offers a set of advanced features like route, holding and speed advices, calculation of take-off times for short-route flights and what-if probing. These advanced features allow to decrease holding, low level vectoring and consequently delays to a minimum. Thus, it will greatly benefit the environment in terms of noise and fuel usage and contribute to cost reductions.

Before considering implementing AMAN or developing its HMI, additional studies are required. Firstly,

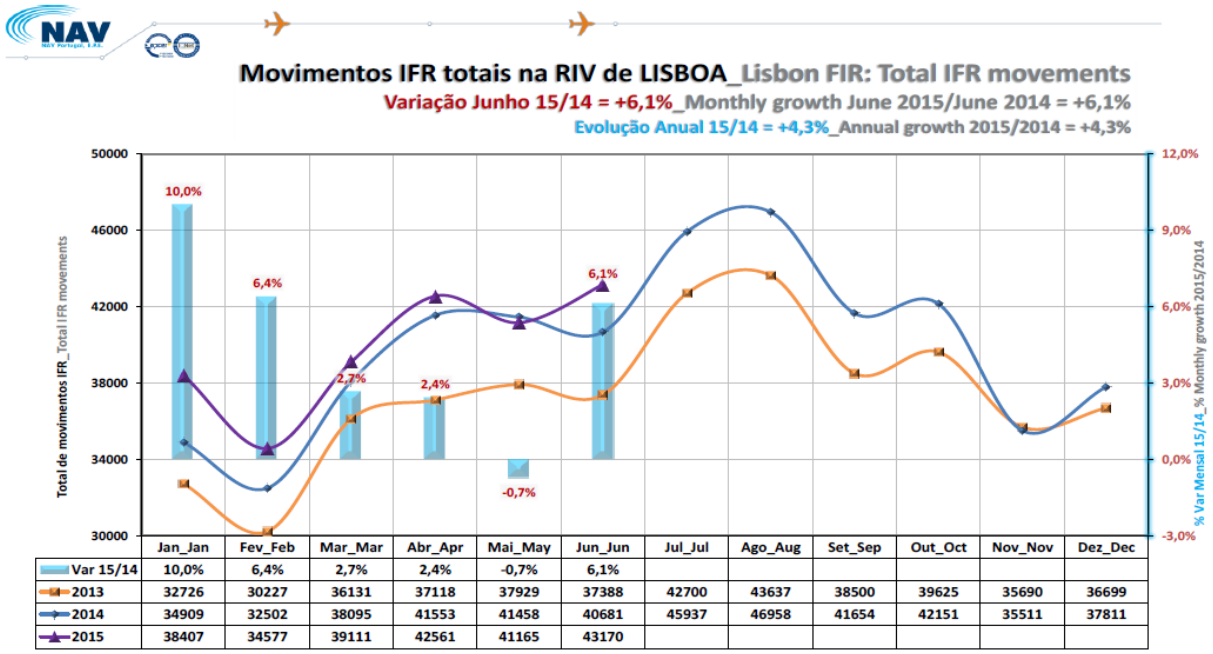

	Jan_Jan	Fev_Feb	Mar_Mar	Abr_Apr	Mai_May	Jun_Jun	Jul_Jul	Ago_Aug	Set_Sep	Out_Oct	Nov_Nov	Dez_Dec
Var 15/14	10,0%	6,4%	2,7%	2,4%	-0,7%	6,1%						
2013	32726	30227	36131	37118	37929	37388	42700	43637	38500	39625	35690	36699
2014	34909	32502	38095	41553	41458	40681	45937	46958	41654	42151	35511	37811
2015	38407	34577	39111	42561	41165	43170						

Figure 1.1: Traffic data for Lisbon's FIR in 2013, 2014 and 2015. [2]

it is important to identify the human performance benefits and potential issues in order to facilitate acceptance and a smooth transition and allow for AMAN to be used at its full potential. Also, and more specific to this work, it is essential to ensure that all prerequisites and particularities of this new software already exist and are operational before considering integrating them.

ATM is a system composed of many interacting elements: people, procedures and equipment. Implementing a software system element such as an AMAN needs to consider all these elements. The airspace and environment in which AMAN will be used and the procedures for its use have to be considered either previously or at the same time. [3]

1.2 Topic Overview

This work is centralized on the parameterization of the prerequisites involved in the operation of an AMAN system to the TMA, a designated area of controlled airspace surrounding an airport.

The OSYRIS AMAN has several inputs. It receives the flight plan data from a Flight Data Processing System (FDPS) and the radar data from a Surveillance Data Processing System (SDPS), and correlates the two. It also utilises an aircraft performance model on its calculations and it is fed with known airspace and flight constraints. Weather and wake turbulance category information is also taken into account. Additional information regarding separation minimums and runway constraints are added manually. Furthermore, optimisation modules can be locally developed and integrated. All the input is processed in a trajectory predictor and an estimated time of arrival (ETA) is computed. The sequencer then builds an organized list of influx into a runway or a fixed point, generally according to the "first come, first serve" criteria. Figure 1.2 is the schematic representation of this system.

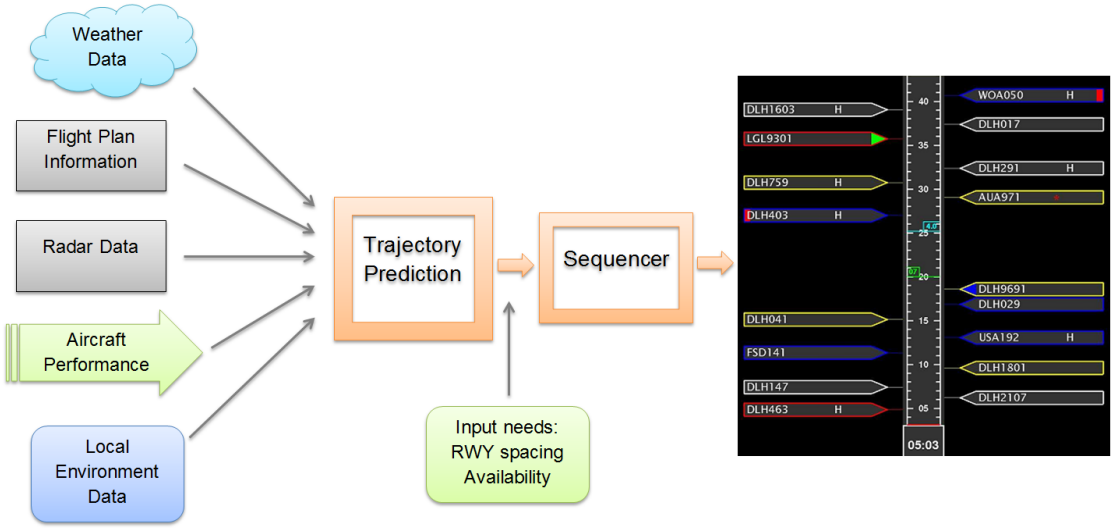

Figure 1.2: Schematic overview of the OSYRIS AMAN system.

The fixed routing for a flight is defined in three stages: departure, en-route and approach/landing. The departure is defined by a Standard Instrument Departure (SID) route and the en-route phase is defined by a set of fixed waypoints for the aircraft to follow. The landing stage is defined by either a Standard Terminal Arrival Route (STAR) or a merging point, according to the method employed in the TMA. AMAN makes use of this information to estimate a time of arrival.

This work studies aircraft's behaviour inside the TMA. More specifically, how aircrafts behave when approaching the airport for landing.

An analysis methodology was developed and a program in Python was created to apply it on a data set. The data includes radar and flight plan information from the months of March, April and May on Lisbon's FIR. The program can run for any other data as long as the parsing and loading steps are done as described in chapter 3.

1.3 Objectives

The purpose of this project was to create a tool that provides real quantified and visual data of flights towards current airspace structures inside TMA sectors.

Ultimately it aims to assist airspace designers, airspace planners, controllers and the AMAN development team to come together and best redefine this sector, if need be. Whether it is to futurely best integrate AMAN into the system or to simply create a more efficient, flexible and dynamic airspace structure.

1.4 Thesis Outline

Chapter 2 provides a review on the state-of-the-art of this work. The Airspace Design activity within EUROCONTROL is explained. Regarding arrival procedures, there are several methods for channeling aircrafts to a runway. These come detailed in this section.

On Chapter 3 the methodologies developed are explained. A detailed description of how these were implemented through Python programs and applied to the data set is given.

Chapter 4 consists on a presentation of the results for all the tests, and for several different scenarios. These were chosen aiming to be able to conclude on and compare the methods described in Chapter 2.

On Chapter 5, conclusions on the different scenarios presented and achievements reached with this work are listed. A section dedicated to recommendations supports a personal opinion on what the optimal solution for Lisbon's TMA sector would be. Suggestions for future work are also given.

Appendix A contains program's output files and additional information to the results presented in Chapter 4.

Chapter 2

State-of-the-art

When flying an aircraft through the sky, pilots follow pre-planned routes, much like highways on the ground. These are ATS routes, specific routes designed for channelling the flow of traffic as necessary for the provision of air traffic services. The term ATS route can stand for any airway, arrival or departure route, among others.

EUROCONTROL is working with the European Comission member states ANSPs and airlines to develop a more rational route network so that flights can go to their destination more directly, saving both time fuel and money. Together they are implementing a flight efficiency plan wich has been agreed to Europe wise. It goes without saying that using less fuel is good for the environment as fewer aircraft emissions are produced. EUROCONTROL helps coordinate the Airspace Design activity.

Today, the Airspace Design activity helps ANSPs to develop, coordinate, validate and implement proposals to optimise Europe's airspace structure, for both en route and terminal space. The objective is to create an efficient, flexible and dynamic airspace structure. The latter needs to accomodate future air traffic demand and meet the SES Performance Scheme's requirements in terms of capacity and flight efficiency, in a cost-effective manner. In Lisbon's FIR, in the upper airspace (245FL upper), Free Route has already been employed and is currently in use.

The Airspace Design activity begins with broad operational requirements that are gradually refined into specific airspace proposals for implementation. The first step is to identify the current and potential problems and their causes.

2.1 Terminal Manoeuvring Area (TMA)

The TMA sector is a designated area of controlled airspace surrounding an airport.

Regarding incoming traffic, there are several methods that can be employed for channeling aircrafts to a runway. Different methods imply different structuralization of the sector.

In 2.1.1 is described the most common structure and the one currently used in Portugal which is using a set of fixed routes called STARs. A more sophisticated system called Point Merge comes described in 2.1.2. Recent work introduced a new concept of integrating tactical shortcut options into the STARs.

This concept is discussed in 2.1.3.

All the methods and structures presented in this chapter are eligible to be integrated into the AMAN system.

2.1.1 Standard Arrival Routes (STARs)

A STAR is a standard ATS route identified in an approach procedure by which aircraft should proceed from the en-route phase to an initial approach fix. STARs were created with the object of safe and efficiently expedite flow of air traffic operating to an airport. They aim to deconflict traffic by the use of specific routings, levels and check points. Each runway should have a number of STARs that ensures that air traffic is not unnecessarily delayed by deviation from its route.

Lisbon's TMA, for example, has 30 different RNAV equipped STARs currently operating. Figure 2.1 shows a fragment of one of the aeronautical charts related to LPPT. This chart in particular illustrates the 7 south entrance RNAV STARs landing at RWY 3 or 35. These are: BUSEN9P, EXONA5A, GAIOS5A, LIGRA5A, NAKOS5A, TROIA5A and UNPOT5A.

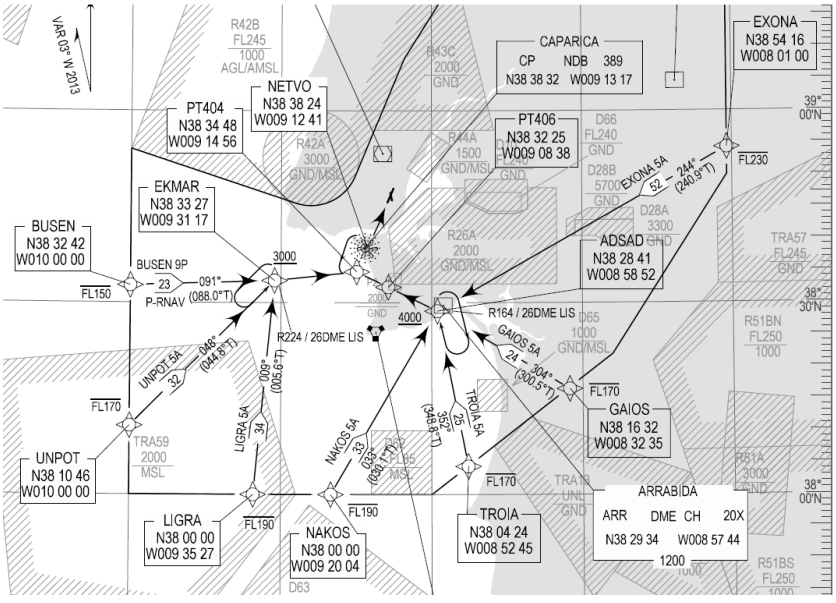

Figure 2.1: The 7 south entrance STARs for RWYs 3/35 at LPPT. [4]

A STAR is assigned to a flight mainly according to its route, i.e. according to the area where it will enter the TMA. Another factors such as weather conditions, type of aircraft and runway in use are also taken into account.

Prior to take off, every flight has a flight plan. However, the STAR field is a lot of the times left empty. In Portugal, when the flight enters the destination FIR, a STAR is automatically assigned to it by the LISATM system. The controller can then transmit that information to the flight or not. If the controller does not follow the automatic attribution by LISATM, this information can not be updated into the system, i.e. if the controller assigns a different STAR to the flight, the STAR field in the flight plan is not updated.

2.1.2 Point Merge

"Terminal Control (TC) Approach operations currently employ "Open-loop" techniques to sequence and space the arrival traffic. This entails the use of tactical vectors: heading, speed and vertical altitude intervention, to merge traffic onto the line of the Final Approach ILS (Instrument Landing System). Point Merge is an innovative method developed by the EUROCONTROL Experimental Centre (EEC) for merging arrival flows with existing technology, including the support of an AMAN. Under a Point Merge System, the aircraft are merged to a point using "Closed-loop" techniques."[5].

The Point Merge method is outlined in Figure 2.2. Incoming traffic is placed onto defined arcs, every point on which is equidistant from the runway. When cleared for landing, the aircraft make one single turn and fly a continuous descent to the runway. At the merging point, the sequence is already integrated.

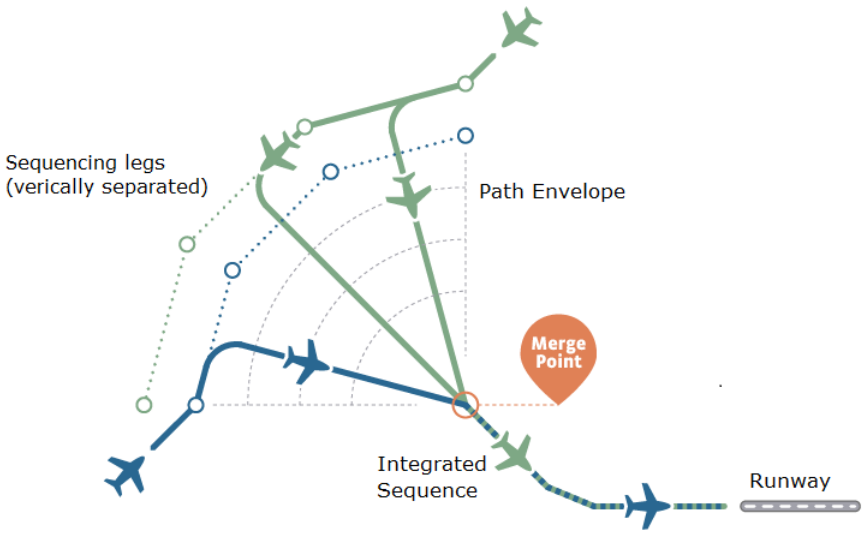

Figure 2.2: Point Merge. [6]

Point Merge was developed in 2006 and is now operational in Oslo (2011) and three Norwegian regional airports (2014), Dublin (2012), Seoul (2012), Paris ACC (2013), Kuala Lumpur (2014), Lagos (2014), Canary Islands (2014) and Hannover (2014).

An independent analysis conducted by NATS (UK Air Navigation Service Provider) established that this system has provided savings of €5.5 million to airlines flying into Dublin Airport during 2013. Per flight, the airlines saved 127kg of fuel, worth €93.10, reducing the fuel requirements in 19.1%. It also found that aircraft reduced the length of the flight by 11.3 miles, a 17% saving. Point Merge also provided savings of 23,500 tons of CO2, representing a 19% reduction. [7]

This system eliminates the need for vectoring or stacking, reduces the need to place aircrafts into traditional holding patterns and the continuous descent approach allows for more efficient fuel usage. If there is a runway congestion, the system holds the aircrafts at much higher altitudes in the linear arcs which consequently decreases fuel burn. From the controller viewpoint, they can also benefit from

enhanced situational awareness and reduced radio frequency transmissions, both of which increasing availability for tactical instructions.

2.1.3 Tactical Shortcut Options

More recent work introduced the concept of using tactical shortcut options to improve schedule conformance in the TMA.

This concept consists of having a dynamic airspace structure for the TMA: longer and shorter nominal paths. If the airspace is less congested, aircrafts are scheduled the shorter paths. When a destination is congested, aircrafts are assigned the longer paths, holding the shorter paths for tactical use when an aircraft is late.

Every flight has a scheduled time of arrival (STA) at coordination points along its nominal route. With the use of an AMAN, the STAs are spaced at a given point to achieve the minimum required spacing plus an additional scheduling buffer to account for uncertainty. The tactical shortcuts are assigned to late aircrafts at some point prior to a coordination point.

This concept claims that using fixed paths produces more accurate trajectory predictions. On the other hand, speed controlling is more efficient fuel wise than vectoring. Using fixed paths and speed control options, a more precise scheduling and tighter spacing is achieved. Though reducing flexibility, it ultimately increases throughput.

On June 2015 in the 10th USA/Europe Air Traffic Management Research and Development Seminar held in Lisbon, a presentation was made on the topic. [8] The work presented not only simulated the concept for the LAX airport, it also enhanced on this concept by adding a mixed aircraft performance model: attributing the shorter path to aircraft equipped to achieve a high degree of schedule conformance, under the same conditions a less equipped aircraft would be attributed the longer path.

The LAX TMA's nominal structure simulation can be observed on Figure 2.3. In black are the nominal path routes, equivalent to our STARs, and in yellow the shortcuts. The saved distance for each shortcut is tabulated in the picture.

The usage of tactical shortcut options is yet to be put into practice. However, the simulation has shown that overall this concept is a potential valuable enhancement for scheduling and spacing. The model reduces the scheduling buffers of aircrafts merging points with a shortcut option and aircrafts equipped to assure high schedule conformance. By reducing these buffers, the flights can be scheduled to the shorter paths and into smaller slots. Thereby, throughput is increased without increasing controller workload. However, as the mixed equippage ratio increases, the benefits seemed to diminish.

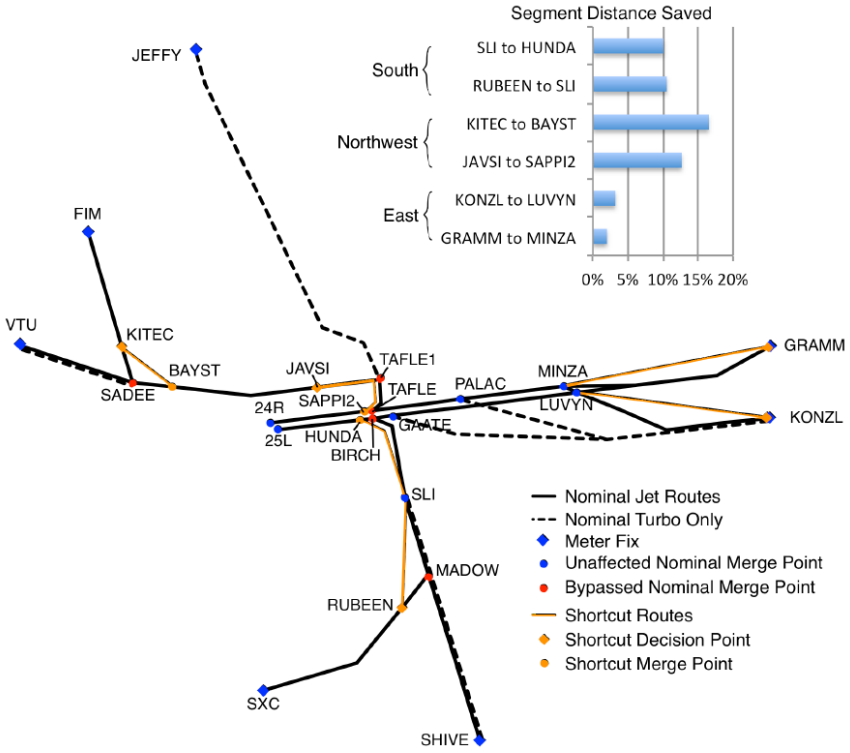

Figure 2.3: Tactical Shortcut Options for the LAX airport.[8]

Chapter 3

Methodology and Implementation

Making a statistical analysis means working with a lot of data. In order to have results in a reasonable timeframe, a strategy had to be outlined. This strategy was to take the raw data, process it, condense it to the essential and save it in a lighter, user friendly way. The program works in two separate steps: The first step is to process and load all needed data into files. Taking the processed data, the second step is to run it through algorithms and produce the desired results.

Before analyzing each step within the program it is important to quickly mention how to obtain the flight data. We were given data from FDPS and SDPS in *rfm* format. This is a proprietary format to store data used by the middleware in LISATM.To convert it to *txt* format, external software already developed at NAV was used. The flight plan data was zipped and ran automatically at once. On the other hand, the surveillance data only ran individual files. A *python* script was created for the application to cyclically parse all the files.

3.1 Loading

With the flight data in a readable format, processing all the information could now begin. Each of the following subsections represent one function of the program.

3.1.1 Settings

The first necessary step was to define a data structure to work with. `Settings.py` defines all global variables and object classes used when data mining. One of the global variables, called *path2project*, defines the directory of the main project. This way the project can be easily adapted to run on any machine or any location within the same machine. This variable is global to the program, hence why `settings.py` is used in every function. The rest of the variables defined here are only used in the loading stage to charge information.

3.1.2 Load

Unlike the first one, `load.py` is an executable function.

This is where the readable flight data is processed and loaded into two GeoJSON files: *DataSurv* and *DataFDPS*. This process can be subdivided in four different stages:

1. `Waypoints.py` extracts information from *pntabs.txt*. This is a configuration file from LISATM that contains every waypoint in Lisbon's and Santa Maria's FIR, including its name and coordinates. Each point is loaded as a Point object and a map of Points (pointsMap) is created.

2. Likewise, `sidsAndStars.py` extracts data from *SidsStars.txt*. This is another configuration file from LISATM, last updated on February 2015, that contains all information about SIDs and STARs. All STAR points are loaded into an object with the same name and a map of STAR points is created (starPointsMap). With this, each STAR is loaded into a STAR object and a STARs map is created (starsMap). Each element in a starMap is a STAR object with all the information regarding the STAR, including its points.

The generated maps (pointsMap and starsMap) are independent to the flights. As so, they are saved in virtual memory and used throughout processing the flight data. In order to be able to use this information outside this function, the maps were also loaded into physical memory. Two GeoJSON files with the names waypoints and stars(ICAO code for the airport) can be found in the ShapefilesList folder, e.g. for Lisbon's airport starsLPPT is created.

The next step was getting the specific data for each day.

Each flight is assigned a *Call Sign* and a *Flight Plan Key*. The combination of these parameters is the key used to distinguish flights within the same day. Data mining is then a process of reading the files line by line and attaching this information to the object with the respective key. This ensures that there is no overlapping data. By the end of one day's reading, a map of objects is saved in virtual memory, each object representing one flight. Adding to the object information is the correlated general data in virtual memory (pointsMap and starsMap). This improved new map is finally loaded in to physical memory through a GeoJSON file.

3. This method is firstly applied for the surveillance data with `surveillance.py` and *DataSurv.geojson* is created.

4. The flight plan data is then parsed by `fdps.py` and *DataFDPS.geojson* is created.

There is one Data(Surv/FDPS) file for each day and each feature within a file represents one flight. The flights are filtered so that only the ones landing at the desired airport are loaded. Figure 3.1 illustrates portions of the generated files for Lisbon's airport on 2015/03/01. Both images correspond to the 8290752 TAP447 flight and, as can be observed, this is the "Feature id" used to identify this particular flight. In DataSurv the coordinates are real data captured by radars along its trajectory. In DataFDPS the coordinates correspond to the fixed waypoints that define the route. Hence why, DataSurv has more

coordinates and they are all more accurate than the FDPS ones. In DataFDPS all the elements starting with ”Points” are information withdrawn from pointsMap.

The main loading function `load.py` runs the four subfunctions, one at a time. Since the data is organized and loaded into physical memory, `load.py` only needs to be executed once.

Shapely and QGIS

The geojson format was deliberately chosen due to two other tools: **Shapely** and **QGIS**. Shapely is a Python package for manipulation and analysis of geometric planar objects. Geojson files can be easily read and loaded into shapes using this package. This will be a great advantage on the testing phase. QGIS is a free and open source application to display geographic information. It provides data viewing, editing, and analysis capabilities. The geojson files can automatically be loaded into GIS and an interactive geographical display of them is made possible.

3.1.3 Correlated Data

When the testing phase began, there was a need to seek surveillance and flight data as well as STAR's data, all in different files. For each flight, three different files were opened, read and matched the correspondant data to the flight, so that the algorithms could be processed. To further improve efficiency, `corData.py` was created.

This is an executable data mining function. It starts off by reading the DataSurv file one flight at a time. With each flight's ”id”, it seeks for the matching information on the DataFDPS file. Having found that, it then seeks the STAR information for the STAR on its flight plan data on the stars(ICAO code for the airport) file. The gathered data is finally dumped into a file with the name corData(date).

Since a lot of the parameters saved in previous files were not useful for the purposes of this work, the dumped data is condensed to its essential. A portion of the corData file describing the same flight as in Figure 3.1 is represented in Figure 3.2. Taken from DataSurv are the real trajectory's geometry, the Track Number, the Time of Day (TOD) and the Aircraft Type. From DataFDPS is the assigned STAR, complemented by the STAR's data. Since the analysis is on the TMA sector, the FDPS route was no longer relevant and the trajectory stored only includes coordinates that intersect it.

The corData(date) files are stored in the folder corDATA. Thus, once these are obtained, if one desires to carry out tests on different machines, one can transfer the program without the heavy DATA folder.

3.2 Getting Results

Once the loading phase was complete, any test could now be executed. Tests are the different analysis made to the data. Each of the following subsections represent a different test and therefore a different function.

```
}, {
    "type" : "Feature",
    "id" : "8290752_TAP447",
    "geometry" : {
        "type" : "LineString",
        "coordinates" : [[-4.888707, 41.77776, 390.0], [-4.899774, 41.774204, 390.
    },
    "properties" : {
        "AircraftType" : "A321",
        "Vy" : ["-84.25", "-84.25", "-84.5", "-84.25", "-84.25", "-84.25", "-84.5"
        "X" : ["", "352700", "351788", "", "349967", "", "348151", "347244", "", "
        "FPL Key" : "8290752",
        "Track Number" : "3811",
        "Y" : ["", "342814", "342356", "", "341464", "", "340564", "340102", "", "
        "f_tod" : ["07:34:59.132", "07:35:03.929", "07:35:08.734", "07:35:13.531",
        "CallSign" : "TAP447",
        "Heading" : ["246.659895", "246.633179", "246.571307", "246.633179", "246.
        "Rate Of Climb" : ["0", "0", "0", "0", "0", "0", "0", "0", "0", "0", "0",
        "TOD" : ["07:34:59.132", "07:35:03.929", "07:35:08.734", "07:35:13.531", "
        "TSE" : ["", "", "", "", "", "", "", "", "", "", "", "", "", "", "", "", "
        "Barometric Height" : [390.0, 390.0, 390.0, 390.0, 390.0, 390.0, 390.0, 39
        "f_cfl" : ["", "", "", "", "", "", "", "", "", "", "", "", "", "", "", "",
        "Long" : [-4.888707, -4.899774, -4.91098, -4.922202, -4.933333, -4.944518,
        "Vel" : ["212.651417", "212.421897", "212.521175", "212.421897", "212.1924
        "RWY Designation" : "",
        "Destination AP" : "",
        "Vx" : ["-195.25", "-195", "-195", "-195", "-194.75", "-194.75", "-194.75"
        "modeC" : [390.0, 390.0, 390.0, 390.0, 390.0, 390.0, 390.0, 390.0, 390.0,
        "Lat" : [41.77776, 41.774204, 41.770486, 41.766914, 41.763255, 41.759634,
    }
}, {
```


(a) Surveillance (Surv)


```
}, {
    "type" : "Feature",
    "id" : "8290752_TAP447",
    "geometry" : {
        "type" : "LineString",
        "coordinates" : [[-1.51, 43.47], [-1.6, 43.4], [-4.11, 42.03], [-5.64, 41.53], [-6.28, 41.1
    },
    "properties" : {
        "Points Z" : ["390", "390", "390", "390", "390", "311", "274", "0"],
        "CallSign" : "TAP447",
        "Points Lat" : ["43.47", "43.4", "42.03", "41.53", "41.17", "40", "39.82", "38.77"],
        "STAR" : "INBOM3B",
        "Points History" : ["121121", "", "TABANERA DEL CERRATO VOR-DME", "ZAMORA DVOR-DME", "SWFAE
        "SID" : "",
        "Points FIR" : ["", "", "", "", "LECM", "", "", ""],
        "Plan Number" : "126",
        "Points Name" : ["BTZ", "", "NEA", "ZMR", "ARDID", "INBOM", "", "LPPT"],
        "Points Y" : ["549681", "541668", "374396", "312988", "271442", "137820", "117161", "1018"]
        "LastReport GlobalData" : ["1425197030", "2015/03/01", "08:03:50,000", "2158", "4028", "274
        "Points UTC" : [["1425193884", "2015/03/01", "07:11:24,000"], ["1425193928", "2015/03/01",
        "Points Remarks" : ["", "", "", "", "", "", "", "AEROPORTO DE LISBOA"],
        "Points X" : ["618121", "611499", "416868", "292245", "239853", "71523", "61890", "579"],
        "Flight Level" : "0.0",
        "FPL Key" : "8290752",
        "Points Aerodromes" : [["", "", ""], "", ["", "", ""], ["", "", ""], ["", "", ""], ["", "",
        "UTC GlobalData" : ["1425195900", "2015/03/01", "07:45:00,000", "", "", "", ""],
        "Points Attr" : ["69", "", "69", "69", "70", "73", "", "65"],
        "Points Type" : ["67", "", "67", "67", "67", "67", "", "67"],
        "Points Situation" : ["'P'", "'P'", "'P'", "'A'", "'A'", "'A'", "'A'", "'A'"],
        "Points Sectors" : [["", "", ""], "", ["", "", ""], ["", "", ""], ["NO", " ", " "], ["TM",
        "Points Priority" : ["3", "", "5", "3", "3", "5", "", "3"],
        "Points CoordRef" : ["65", "", "65", "65", "65", "65", "", "65"],
        "Route GlobalData" : ["1425198118", "2015/03/01", "08:21:57,620", "", "", "", ""],
        "Points Long" : ["-1.51", "-1.6", "-4.11", "-5.64", "-6.28", "-8.3", "-8.42", "-9.13"]
    }
}, {
```


(b) Flight Plan (FDPS)

Figure 3.1: Portions of the Data files for Lisbon on 2015/03/01.

```
}, {
    "type" : "Feature",
    "id" : "8290752_TAP447",
    "geometry" : {
        "type" : "LineString",
        "coordinates" : [[-9.136569, 38.779909, -0.75], [-9.135218, 38.782505, -0.75], [-9.1338
    },
    "properties" : {
        "AircraftType" : "A321",
        "STAR" : {
            "type" : "Feature",
            "id" : "INBOM3B",
            "geometry" : {
                "type" : "LineString",
                "coordinates" : [[-8.301944444444445, 40.00194444444445], [-8.4925, 39.66555555
            },
            "properties" : {
                "Points Names" : ["INBOM", "FTM", "RINOR", "PT410", "PT411", "UPKAT", "THR21"],
                "Heights" : [[55, 270], [70, 245], [70, 245], [40, 245], [40, 245], [40, 245],
            }
        },
        "CallSign" : "TAP447",
        "Track Number" : "3811",
        "TOD" : ["08:17:31.234", "08:17:26.429", "08:17:21.632", "08:17:16.835", "08:17:11.734"
        "FPL Key" : "8290752",
        "Date" : "20150301"
    }
}, {
```


Figure 3.2: Portion of the corData file for Lisbon on 2015/03/01.

There are three main tests: **Adherence**, **Average Stars** and **Point Direct**.

The Adherence, as the name suggests, tests real trajectory's adherence to its assigned STAR. The method used was to draw a buffer around a STAR and calculate the length of the track that intersects this buffer. The STAR's adherence is proportional to the fraction between the intersected track length and the STAR's total length. Figure 3.3 is a QGIS representation of TAP473's flight on the INBOM3B STAR using a 2nm buffer radius. This test was made in two phases. In 3.2.1 comes the 2D Adherence and in 3.2.2 the 3D Adherence.

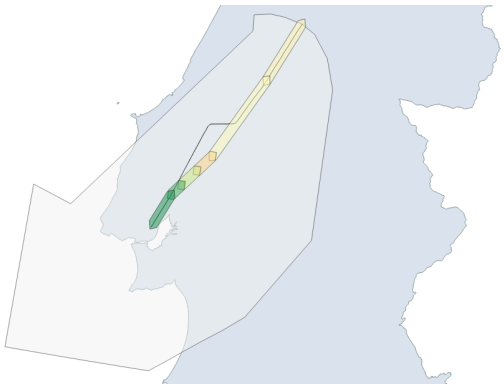

Figure 3.3: TAP473 flight on the INBOM3B STAR on 2015/04/25.

Given its results, two additional tests occurred. The first one infers about real trajectory STAR patterns. It was named Average STAR and comes detailed in 3.2.3. Point Direct steps in for cases where the real trajectory patterns resemble a Point Merge operation. Its algorithm comes detailed in 3.2.4.

3.2.1 2D Adherence

The first test to be made was a two dimensional adherence test.

Relying on the shapely tools, a buffer is drawn around the STAR. The STAR's adherence rate is directly proportional to the portion of the trajectory that intersects that buffer. The buffer is set on a scale of one nautical mile and goes from 1 to 5nms to each side.

In addition to the analysis of the adeherence to the STAR in its entirety, the STAR was also broke into segments. Each segment joins two consecutive points of a STAR. The adherence for each segment is tested using the same methodology as for the entire STAR.

During the flight, pilots receive instructions from the ATC and the STAR initially proposed in the flight plan is often changed. However, these changes are not updated nor recorded. In these cases, since the performed STAR is not the one on the FP, the adherence rates are a lot lower than expected. Because this was a recurring situation there was a need to conduct a correction.

The `corData2D.py` function analyzes a number of criteria relating to the flight plan STAR and keeps these results. It then goes on analyzing the same criteria for all the remaining STARs. If all the results are favorable to a different STAR, an illation is taken about there being a correction. If so, this becomes a flight that has been ”corrected” and the results for the new STAR are taken into account. These correction parameters are specified in the pseudo code presented in Algorithm 1.

Algorithm 1 STAR's Correction function.

```
1:
2: function GETCORRECTIONSTAR(STARFP)
3:
4:     seg1FP = Adherence to the 1st segment of the starFP
5:     starFPlen = Adherence to the starFP in length
6:     resFP = seg1FP * starFPlen + buffer for uncertainties
7:
8:     for star in listAllStars do
9:         seg1 = Adherence to the 1st segment of the star
10:        starlen = Adherence to the star in length
11:        res = seg1FP * starFPlen
12:
13:        if res > resFP then
14:            newStarsList ← star
15:
16:    if newStarsList == {} then return starFP
17:
18:    else return star with most similar shape to the track
19:
```

The algorithm for the 2D adherence function comes simplified in 2.

Algorithm 2 2D Adherence.

```
1:
2: function GETADHERENCE(shape, track)
3:
4:     buffedShape = shape.buffer(2nm)
5:     intersectedTrack = track.intersection(buffedShape)
6:     numerator = intersectedTrack.length
7:     denominator = buffedShape.length
8: return numerator/denominator
9:
10: function GETRESULTS(star)
11:
12:     resSTAR = GETADHERENCE(star, track)
13:     resSEGMENTS = list()
14:     for resSEGMENTS in star do
15:         resSEGMENTS.append( GETADHERENCE(segment, track) )
16: return resSTAR, resSEGMENTS
17:
18:
19: function MAIN()
20:
21:     for flight in CORDATA do
22:
23:         starFP = flight['properties']['STAR']
24:         resultsFP = GETRESULTS(starFP)
25:
26:         starCorrected = GETCORRECTIONSTAR(starFP)
27:         resultsCorrected = GETRESULTS(starCorrected)
28:
```

To save and present the results two platforms were chosen: **PDF** and **QGIS**. To generate the files two external functions `pdf_2D_3D.py` and `qgis_2D_3D.py` run internally in the main program `cordata2D.py`.

Three **PDF** files are generated. Two of them present the adherence rates for the entire STAR and for each segment of the STAR and the number of flights analyzed per STAR. The first of the two being the results without any corrections made, i.e. the rates and number of flights for the STARs in the FP. The second one assumes corrections might have been made. It is identical to the first one except that results are for the ”most favorable” STAR. Thus one obtains higher rates and in general higher range of STARs. Finally the third file gives global information and compares corrected to uncorrected results. It presents the overall adhesion rate and the number of flights for both cases. It also contains a table that allows us to infer about correction patterns by STAR. That is, for a given STAR, how many flights were corrected and to what new STAR.

As for **QGIS**, the function generates one file for each uncorrected STAR. Within each one, one can observ the STAR's buffers, full and partial (segments) and the aircraft's trajectories. If, for that STAR, there are trajectories that have been corrected, the same shapes can be found on Tracks $>$ Corrected. To better situate the STAR's and trajectories, the background is the map of Portugal overlapped with a transparency that corresponds to the TMA sector.

Everything is presented stereographically on the QGIS files and they are also interactive. One can select which tracks or portions of the STAR wiches to see. Also, by clicking a selected component with the information cursor it has access to additional information about that specific component.

In both data viewing platforms, the results follow a diverging colormap that goes from red to yellow to green. This is intended to give a better perception of the divergence of the results. The green end represents 100% adherence and the red one represents 0% adherence as ilustrated in Figure 3.4.

Figure 3.4: Colormap percentage scale.

To perform the 2D adherence test, the user must select *a priori* three parameters:

- The minimum scale of analysis is the day. The user can then analyze any day from the loaded days. Alternatively, it can choose a combination of these days: one week, every Monday, one of the months: the combinations are numerous. For this purpose, the variable **criteria_list** should be amended to contain all desired days prior to running the function.

- Then the user must choose the name of the folder where the files will be stored in. This folder will be stored in RESULTS. The variable **file_out_name** is the one to customize. If there is already a folder with that same name in the directory, the old one will be completely removed and the new one is stored with new results. To this name the test type and the buffer radius are added, e.g.: 2D_(foldername)_2NM.

- Finally, the user must select the buffer **radius**: 1, 2, 3, 4 or 5 nautical miles.

`corData2D's` last lines are displayed in Figure 3.5. Here is where the parameters are chosen according to the desired test.

```
# Criteria Options: 'mon','tue','wed','thu','fri','sat','sun',
#                   'march','april','may',
#                   (singleday) e.g.: '20150301' (yyyymmdd),
#                   'all'
criteria_list = ['20150301']

# Output file & folder name
file_out_name = '1_March'

# Nautical Miles (1, 2, 3, 4 or 5)
radius = 2
```

Figure 3.5: User's criteria.

3.2.2 3D Adherence

About shapely: *"A third z coordinate value may be used when constructing instances, but has no effect on geometric analysis. All operations are performed in the x-y plane."* [9]

The three dimensional analysis ceases to be as linear as the two dimensional. In 2D, intersecting the track in the buffed shape and getting its length required two shapely functions: intersection and length. In 3D, the exact same functions were used. However, this time it was necessary to do this process twice: once for x-y (2D) and the other time for l-z, l being the length of the track and z its altitude. Getting l-z involved manipulating existing geometric shapes. The end result is an intersection of both plane's results.

Before any operation begins, it was firstly necessary to correct the track's z coordinate for QNH. LISATM's SDPS only receives altitude information from avionics in Mode C, i.e. the altitude with reference to International Standard Atmosphere (ISA). As soon as the track is extracted from the corData file, all the points that lie below the $4000ft$ transition altitude will suffer adjustments. A file with the name qnh.txt in the DataSS folder contains the value for QNH for all the days that were loaded. For each date, the QNH is updated every half hour. Based on the last TOD for the track and the day of the flight, qnh.txt is scanned and the QNH value for that time is extracted. With this value, the adjustments in Equation 3.1 were made. $1013.25ft/hPa$ is the air pressure at mean sea level (MSL) and $30ft = 1hPa$.

$$z = z - (1013.25 - QNH) * 30 \tag{3.1}$$

Then, the algorithm runs as follows. Taking the track corrected for QNH, the STAR is extracted from its flight plan. Taking the first segment of that STAR, a buffer was built around it in 2D. The track is intersected just like it was on the 2D analysis and the portion of the track that intersects that specific segment in latitude and longitude is obtained. Up until this point, the algorithm is identical to the 2D. Now there is a need to know, from that portion of the track, which subportion or subportions also meet the altitude restrictions.

Taking the intersected track, its length is computed and this will be l_{max}. The STAR segment altitude buffer is then created with the configuration displayed on Figure 3.6. The buffer starts at $l = 0$ and ends at $l = l_{max}$. This allows for the entire portion to fit into the buffer. As for z, A and B stand for the two STAR points that make the STAR segment and h corresponds to their height restrictions. For example, h_{max_A} stands for the maximum height for point A.

Each STAR has different altitude restrictions for each point. Because every track's length is different, the altitude buffers will also be different, that is, singular to a specific flight.

Having built the buffer, it is now necessary to create the track to intersect it. This can no longer be the same track portion obtained earlier as its x and y have now to be l and z. An auxiliary line is created. Its y is simply the z coordinates from the track, and x the cumulative length of its points.

Intersecting this new line with the buffer on Figure 3.6, the desired subportion or subportions are obtained.

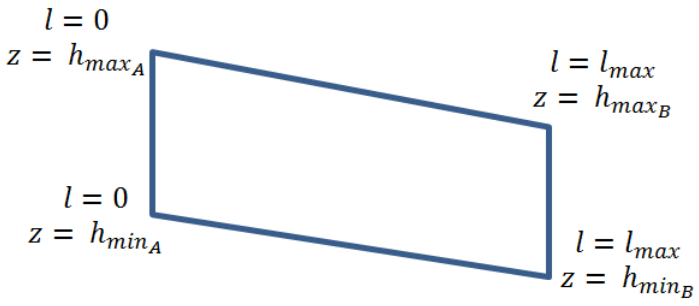

Figure 3.6: Height Polygon

Running this algorithm for each segment of the STAR, a set of track fragments is obtained. These allow for inference about the flight's 3D adherence rate.

As in the 2D analysis, the results are divided on to adherence rates for the STAR in its entirety and for each of its segments. The same inferences were made about ATC corrections.

The same `pdf_2D_3D.py` and `qgis_2D_3D.py` were used and therefore the generated files and their display is identical. Because in QGIS the 3D adherence is not discernible, instead of displaying the entire tracks, as in 2D, only the intersected fragments are displayed, instead of the entire track. This feature can be seen on Figure 3.7 which shows the QGIS geographical represention of flight's TAP447 adherence to the INBOM3B STAR on the 1st of March 2015. This is the flight used as an example in section 3.1. In 2D, the portion of the track that intersects the buffer is visually identifiable. In 3D however, this is not the case and for this reason, only the portion of the track that intersects the buffer in all 3 dimensions is represented. In this case in particular, the aircraft is entering the STAR at a higher altitude than the one regulated.

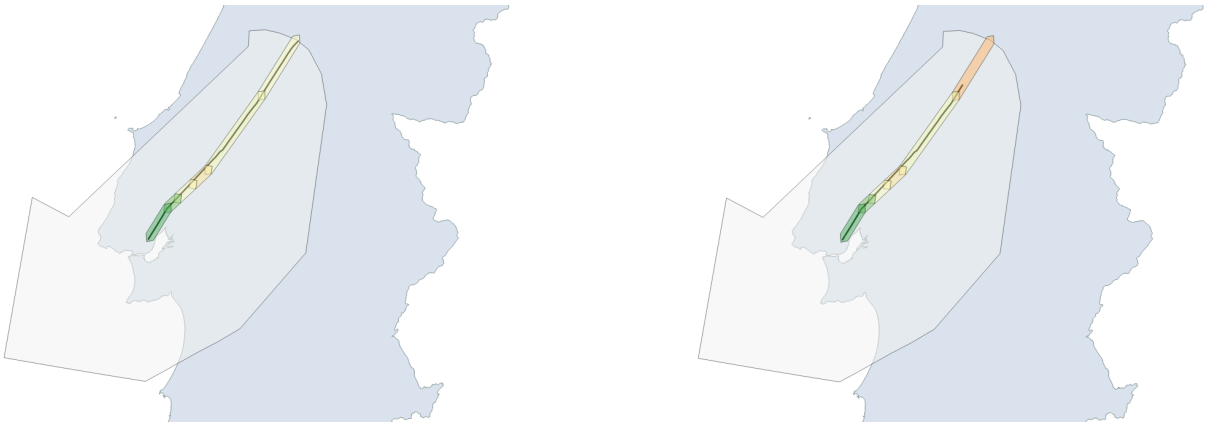

(a) in 2D. (b) in 3D.

Figure 3.7: Geographical represention of flight's TAP447 adherence to the INBOM3B STAR on 2015/03/01

According to the desired study, the same criteria must be defined *a priori* by the user: **criteria_list**, **radius** and **file_out_name**.

3.2.3 Average STARs

Testing the 2D adherence it was visible that aircrafts use shortcut options whenever possible. The segments farther away from the runway often had very low or even nil adherence rates. Even so, tracks managed to keep some kind of pattern.

For these reasons, a new test was thought to be made. `avSTARs.py` aims to trace down common real trajectory patterns for each STAR. Three different patterns were traced, each of them following a different algorithm. The first one is the **Average**, then the **Iterative Weighted Average** and finally the **Median**.

Taking a specific STAR, the program starts by loading all the tracks associated with it. This is the corrected STAR, that is, the STAR that best suits the track, not necessarily the flight plan's STAR.

After loading all the tracks, it then searches out for the track with the least amount of points. Taking this minimum number of points, all the tracks are then normalized into that amount. This means the tracks are divided in equal sized parts so that they all have the same amount of points.

Average

Taking all the first points, the average first point is computed. The average point is the one resulting from the average latitude plus the average longitude from all the points considered. The process is repeated for all the points the tracks were divided into. In the end, all the average points are joint and the average line or track for that specific STAR is obtained.

Figures 3.8, 3.9 and 3.10 demonstrate the process. A sample of four different tracks related to the same STAR were gathered. The segments from two consecutive normalized points from each STAR are presented in Figure 3.8. The average points for each set of track points are presented in red in Figure 3.9. In Figure 3.10, joining these two points, the average line segment is obtained.

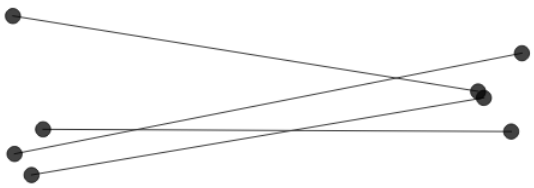

Figure 3.8: Sample of four track's normalized segments.

Figure 3.9: Computation of the average points.

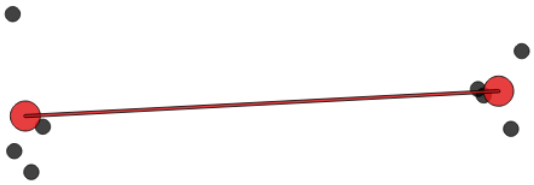

Figure 3.10: Computation of the Average line.

Iterative Weighted Average

Even though the previous test already gave successfull visual results, we wanted to further refine the pattern. For most STARs, tracks did not deviate significantly from the average. However, some STARs had one clear pattern and then a small percentage of tracks significantly different from this pattern. Computing the average was attributing the same weight to the tracks in the clear pattern and the abnormal tracks.

The Iterative Weighted Average test was built. The same normalized tracks and computed average points were considered. Taking all the first points of the tracks, its distance to the average first point is calculated. This time the computed point is the weighted average point. The weights being inversely proportional to the distance of the point to the average point. This process is done iteratively. Taking the new computed point, the distance is again calculated for each point and either is the final weighted average point. The iteration stops when the distance between new calculated points is less than $1m$. This way, the further a certain track is to the average, the less weight it will have on the new line's computation.

Continuing with the same example, in Figure 3.11 there is a visual comparison of the two tests. The red line results from the Average and the green from the Iterative Weighted Average test. With the refined Weighted Average test, the computed line follows the areas with bigger density of points, as desired.

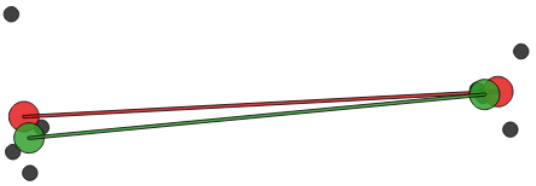

Figure 3.11: Comparison between the Average test in red and the Iterative Weighted Average in green.

Median

Lastly it was noticeable that, although more accurate than the first one, the new test resulted in a very irregular line. Furthermore, the iterations made the program heavy and slow.

In order to surpass these issues, a simpler test came to mind: the Median. Instead of joining the average points, the line is the union of the median points. On Figure 3.12, the similarities between the median in yellow and the weighted average in green are identifiable. This solution results in a much

smoother line and it is faster processing, despite the results being very similar to the last test.

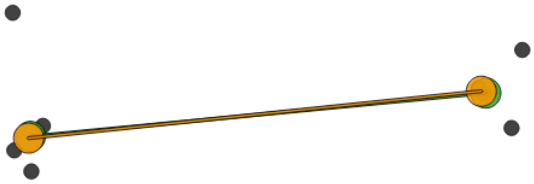

Figure 3.12: Comparison between the iterative weighted average test in green and the median in yellow.

The final results are presented in a different QGIS file for each STAR. The tracks used in the calculations and the tree resulting lines: the average in red, the iterative weighted average in green and the median in yellow, are shown. The tracks used for calculations are the ones with less than 70% adherence to the STAR.

One could call the resulting lines new alternative STARs. An additional study was made on how much of an improvement to the real STAR these lines would be. The 2D adherence was again tested, now for the Average, Iterative Weighted Average and Median "STARs".

3.2.4 Point Direct

On 3.2.3 flight patterns were traced as lines in order to mimic a possible alternative STAR. Analyzing the geographical results and comparing real tracks with their STAR, patterns like the one in Figure 3.13 came up often. In cases like this, the pattern is not best described as a line. Instead, the approach here was to grant pilots a direct flight to a STAR point inside the TMA, resembling the Point Merge method.

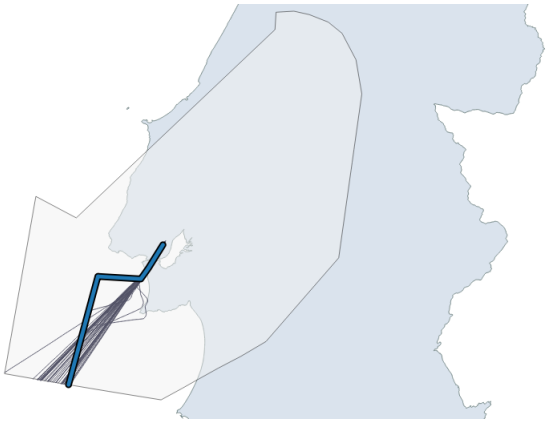

Figure 3.13: Flights on the LIGRA5A STAR in Lisbon's TMA. This screenshot was taken from the Average STARs test. The tracks represented are a sample of 50 of the tracks for this STAR for all the available data.

For these scenarios, `pointDirect.py` was created. The function calculates the number of non conformative aircrafts that were granted a direct-to flight to a STAR point inside the TMA. A non conformative flight was agreed to be one that had less than 70% adherence to its STAR.

The algorithm is as follows. Taking one non conformative flight and its STAR, it checks if the track intersects the STAR's points, starting with the point closest to the runway, one at a time until the penultimate point. If the track is positive to fly by a certain point, directivity is checked, i.e. if the trajectory until that point was a straight line. If it was not, the process is repeated for the next point. If it was, the results are gathered and the test continues for the next track.

In the end, a pdf file can be consulted for results. In a table are presented the number of non conformative flights for each specific STAR and, from those, how many flew directly and to which point. Along side the tabulated data, one can also visualize these flights in the qgis platform.

Chapter 4

Results

For this work were provided 3 months of SDPS and FDPS data: March, April and May of 2015. This data covered Lisbon's FIR which includes the continental area and Madeira.

Because AMAN is to be implemented in Lisbon and the internship was held at NAV's head office in Lisbon, the main results were extracted for Lisbon's TMA. They can be consulted in 4.1. As proof of concept, adjusting some simple parameters, we were able to run the programs for Oporto. The results for this airport can be consulted in 4.2.

With the exception of subsection 4.1.4, all results were obtained using a 2 nautical miles buffer.

Recall the colormap used to represent the percentage of adherence in 4.1.

:

Figure 4.1: Colormap percentage scale.

4.1 Lisbon's TMA - LPPT

The set of results presented in this chapter attempts to portray all different scenarios. The aim is to be able to best compare and contrast all of them and conclude on the topic.

In 4.1.1 is presented the 2D adherence for all the months. 4.1.2 compares the 2D and 3D adherences. In 4.1.3 an attempt was made on tracing a relation between the amount of traffic and the adherence. 4.1.4 explains the buffer radius choice for the tests. In 4.1.5 the resulting patterns for STAR's taken from real data are presented. Finally in 4.1.6, flight's directivity was tested.

4.1.1 2D adherence, all data

The first test was the two dimensional adherence for all the data.

The uncorrected STAR's have an average global adherence of 49%. Assuming the corrections made reflect ATC's intervention, if the flight plan was updated during flight this adherence would increase to

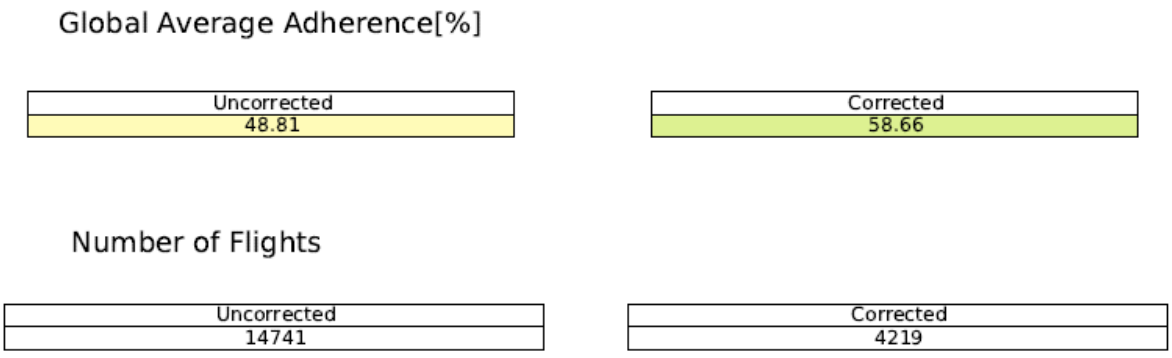

Figure 4.2: Global Average 2D Adherence for LPPT.

59%. This is illustrated in Figure 4.2. In the 3 months analyzed, 18960 aircrafts flew into Lisbon's airport from which 4219 were corrected. In average, there were 206.1 flights per day.

In Figure 4.3 is an example of the output QGIS file for the INBOM3B STAR on the 2015/03/01. On the left one can select the layers to be represented on the map on the right. In this particular case there is the TAP447 flight, used as an example in subsection 3.1.2, on the INBOM3B STAR. The other flight is the RYR530X flight which was corrected to the XAMAX5D STAR. The INBOM3B STAR is represented by segments and the XAMAX5D is represented as the whole. The colors match the average adherences to the segments (INBOM)or the average adherence to the STAR (XAMAX).

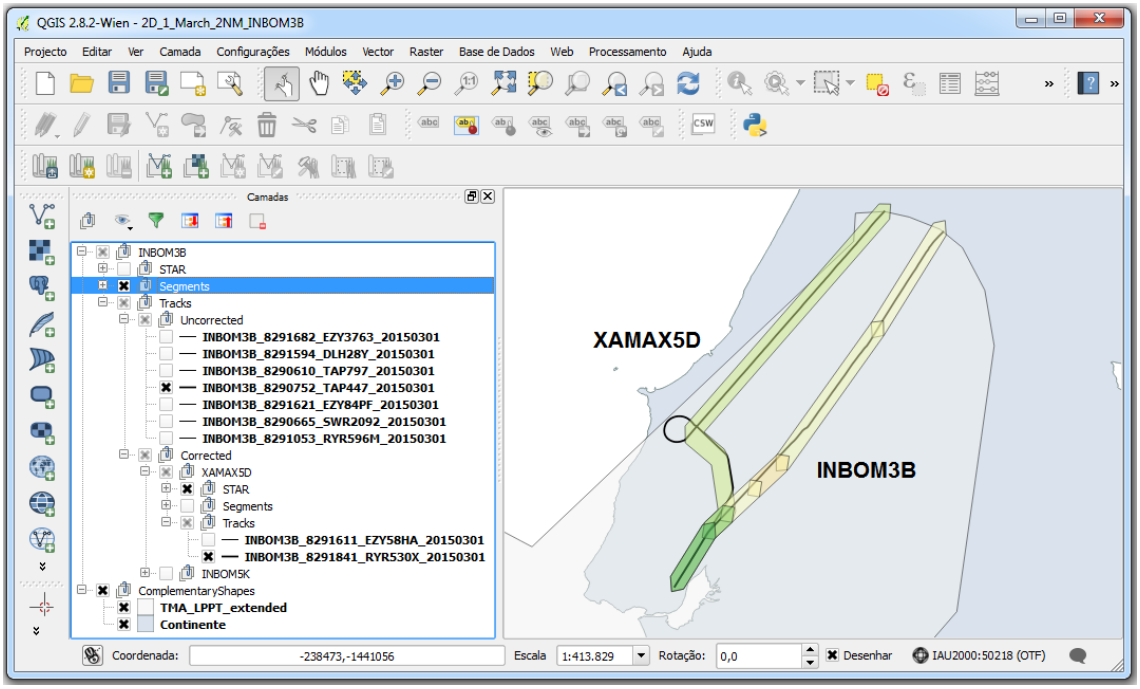

Figure 4.3: Example of the output QGIS file for the INBOM3B STAR on the 2015/03/01.

The detailed results for each STAR come attached in Appendix A, section A.1. The first file is for the uncorrected results and the second one for the corrected.

From this point forward, unless mentioned, the results presented are for the corrected STARs.

4.1.2 2D vs 3D adherence

In this section a comparison is made between 2D and 3D adherences.

The global average adherences for 2D and 3D are presented in Figure 4.4.

(a) 2D (b) 3D

Figure 4.4: Global Average Adherence for 2D and 3D.

In Figures 4.5 and 4.6 comes the tabulated adherences per STAR per segment, the 1st segment being the one closest to the runway.

	1	2	3	4	5	6	7	8	9	10	11	12
GAIOS3B	87.68	52.08	9.80	3.97	1.61	0.14	0.73	0.16	0.00	0.00	0.00	6.82
TROIA3B	91.49	71.31	30.40	4.24	0.80	2.18	2.70	8.71	5.15	3.08		
BUSEN3B	90.60	46.74	5.20	0.72	0.34	3.15	9.36	14.82	6.22	8.61		
NAKOS5A	86.16	73.97	37.88	5.24	12.13							
EXONA3B	89.69	63.18	12.70	6.28	14.82							
UNPOT3D	89.37	43.70	15.47	5.28	29.56	18.92	21.24					
NAKOS3B	90.95	61.30	9.34	3.47	1.97	1.43	11.02	56.38	23.73	15.24		
LIGRA3B	93.14	56.61	11.66	3.86	0.00	2.49	8.49	38.25	40.09	25.31		
GAIOS3D	91.43	50.93	6.95	2.54	49.86	26.17	20.92					
UNPOT5A	85.78	75.39	38.35	15.34								
LIGRA5A	90.51	91.55	21.95	21.86								
BUSEN3D	91.76	60.06	33.38	26.25	32.29	8.86	31.98					
UNPOT3B	95.41	60.98	13.07	5.19	3.94	4.65	16.32	25.20	37.84	61.05		
XAMAX6C	86.61	68.55	29.03	15.00	6.49	45.81	43.62					
XAMAX5D	92.46	68.65	41.77	23.20	36.35							
GAIOS5A	84.92	59.57	35.64	41.48	32.66							
XAMAX3B	91.79	83.43	50.97	20.08	27.70	42.87						
UNPOT3K	85.59	66.90	57.24	27.85								
TROIA3D	92.14	59.25	55.66	60.54	67.02	17.71	8.12					
BUSEN9P	86.44	63.15	33.09	41.94								
TROIA5A	86.37	54.04	45.37	37.83	8.21							
XAMAX5K	83.22	47.99	29.07	51.86	92.08	30.58	31.96					
EXONA5A	83.94	59.09	35.56	25.74	53.46							
IDBID5B	91.20	76.91	33.91	27.96	46.19	57.33						
XAMAX5A	89.85	88.42	59.24	47.56	69.26	87.73	92.23	31.97	30.96			
LIGRA3D	91.99	61.13	18.13	9.31	65.13	59.27	65.93					
INBOM3B	92.25	86.00	69.72	44.06	58.65	60.96						
NAKOS3D	92.18	64.11	51.63	29.05	74.15	64.59	78.50					
INBOM5A	84.93	60.15	21.49	13.85	26.01	62.26	91.62	86.00	67.43			
INBOM5K	84.06	53.98	37.24	58.27	92.66	85.74	78.58					

Figure 4.5: Adherence per STAR per segment in 2D.

The UNPOT3K STAR has 0.12% adherence in the first segment. This is explained by the very narrow corridor regulated for this STAR shown in Figure 4.7.

The detailed results for each STAR for 3D come attached in Appendix A, section A.2. The 2D results are in section A.1.

	1	2	3	4	5	6	7	8	9	10	11	12
UNPOT3K	0.12	34.57	18.26	4.90								
GAIOS3B	86.28	35.46	9.80	3.97	1.61	0.14	0.42	0.00	0.00	0.00	0.00	6.58
BUSEN3B	89.16	36.97	5.20	0.72	0.28	1.50	3.00	3.40	6.09	8.14		
TROIA3B	90.75	63.41	30.34	2.60	0.48	1.48	0.06	5.11	5.10	2.96		
XAMAX5K	78.52	37.23	9.21	5.22	23.49	16.77	0.75					
NAKOS3B	90.14	52.35	9.34	2.72	0.80	1.07	3.12	28.12	23.27	14.93		
LIGRA3B	90.70	46.24	11.66	3.82	0.00	2.49	3.03	16.27	40.09	25.08		
NAKOS5A	86.10	68.04	35.70	5.07	11.97							
EXONA3B	89.43	58.22	12.70	5.49	14.45							
UNPOT3D	89.00	38.48	6.48	3.01	27.41	18.92	20.17					
INBOM5K	79.93	42.75	13.48	7.88	27.17	39.15	0.77					
GAIOS3D	91.44	40.71	0.00	2.31	44.98	26.17	20.92					
UNPOT5A	85.57	69.07	38.18	14.28								
UNPOT3B	91.38	57.11	13.07	4.07	1.89	1.86	4.13	13.75	35.66	57.22		
LIGRA5A	90.21	85.07	21.47	21.83								
BUSEN3D	91.44	55.93	15.97	19.15	30.02	8.86	29.97					
XAMAX6C	86.45	60.94	28.96	14.89	5.42	41.20	39.27					
TROIA3D	92.14	55.48	0.00	35.80	65.21	17.71	8.12					
XAMAX5D	92.22	65.92	30.38	19.54	34.66							
GAIOS5A	84.62	50.20	34.13	41.02	32.18							
XAMAX3B	91.77	80.99	50.91	19.85	27.53	41.25						
BUSEN9P	86.13	54.19	32.73	40.81								
TROIA5A	86.07	47.05	44.83	37.36	7.54							
XAMAX5A	89.68	81.52	59.24	47.02	68.39	87.20	90.74	28.47	12.73			
EXONA5A	83.75	51.82	34.46	25.60	51.19							
IDBID5B	91.01	74.01	33.90	27.30	42.33	40.99						
LIGRA3D	91.99	55.01	3.84	4.08	60.47	59.27	65.93					
INBOM5A	84.68	52.71	21.43	13.63	25.66	58.35	82.42	75.61	24.58			
NAKOS3D	90.77	55.14	20.00	19.89	65.66	60.02	76.32					
INBOM3B	92.08	83.38	69.72	42.98	57.92	56.38						

Figure 4.6: Adherence per STAR per segment in 3D.

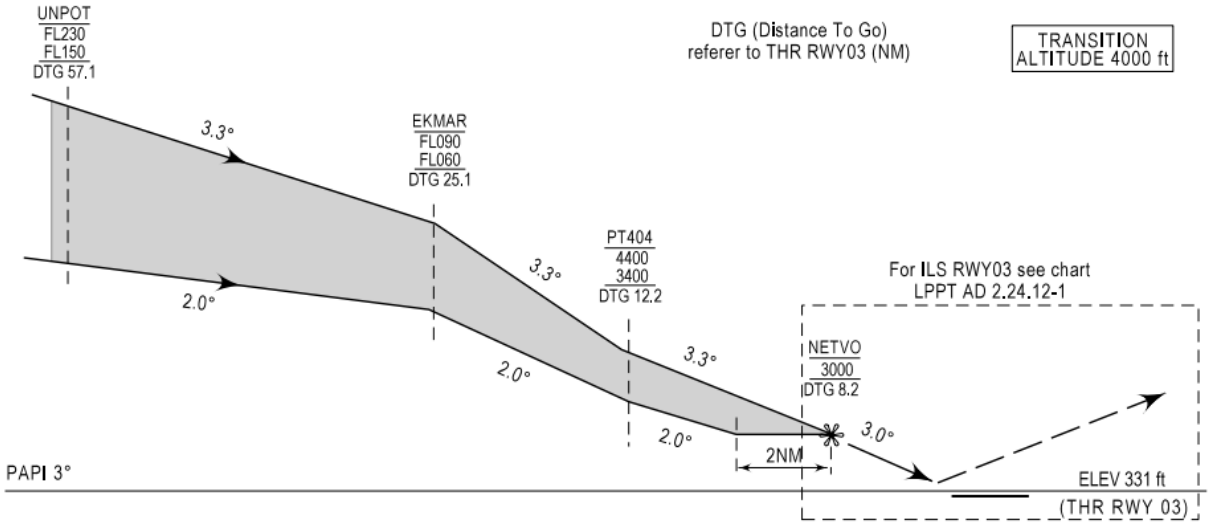

Figure 4.7: UNPOT3K altitude restrictions. [4]

4.1.3 High vs low traffic scenario

A congested terminal area would suggest a higher percentage of adherence. During low traffic periods pilots have more freedom to fly directly without having to follow the specific path.

This study aimed to find the relation between airport's traffic and STAR's adherence. Thereunto, taking the number of flights and the global average 3D adherence for each day, two graphs were produced.

These can be seen on Figure 4.8: a) corresponds to the global average adherence for the data without corrections and b) for the corrected data.

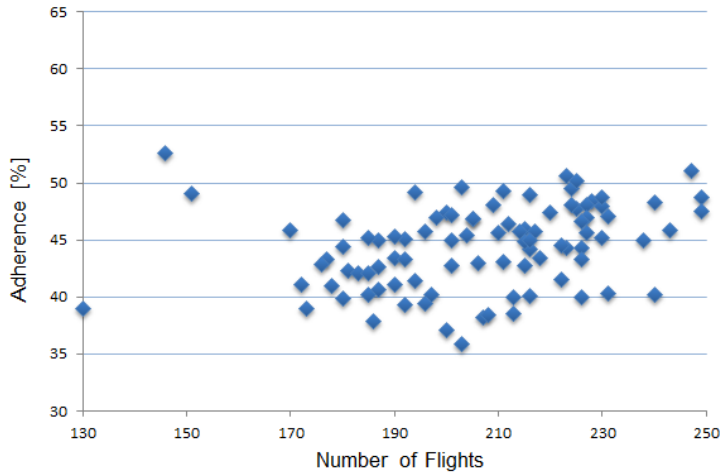

(a) Uncorrected

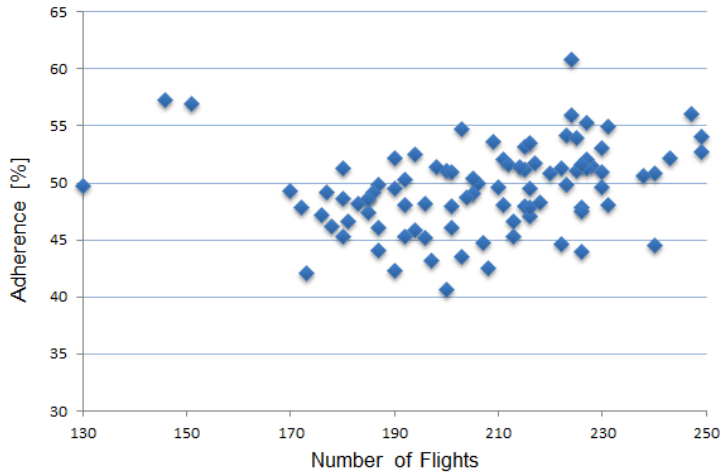

(b) Corrected

Figure 4.8: Number of flights per day vs adherence.

4.1.4 Buffer radius

Augmenting the buffer will evidentely increase STAR's adherence. The idea of this study was to find the best buffer, i.e. the buffer that produces better results without compromising accuracy.

We tested the adherence for the 3 months with the different buffer radius available: 1, 2, 3, 4 and 5nm. The results come in graph form presented in Figure 4.9. Each line corresponds to a different STAR and the graph confronts buffer radius with adherence.

The idea behind this graph was to visually calculate the area below each line and sequence the STARs by decreasing area. From top to bottom, on the figure, comes the sequence. Choosing the buffer would be a question of identifying which buffer produced the most similar sequence.

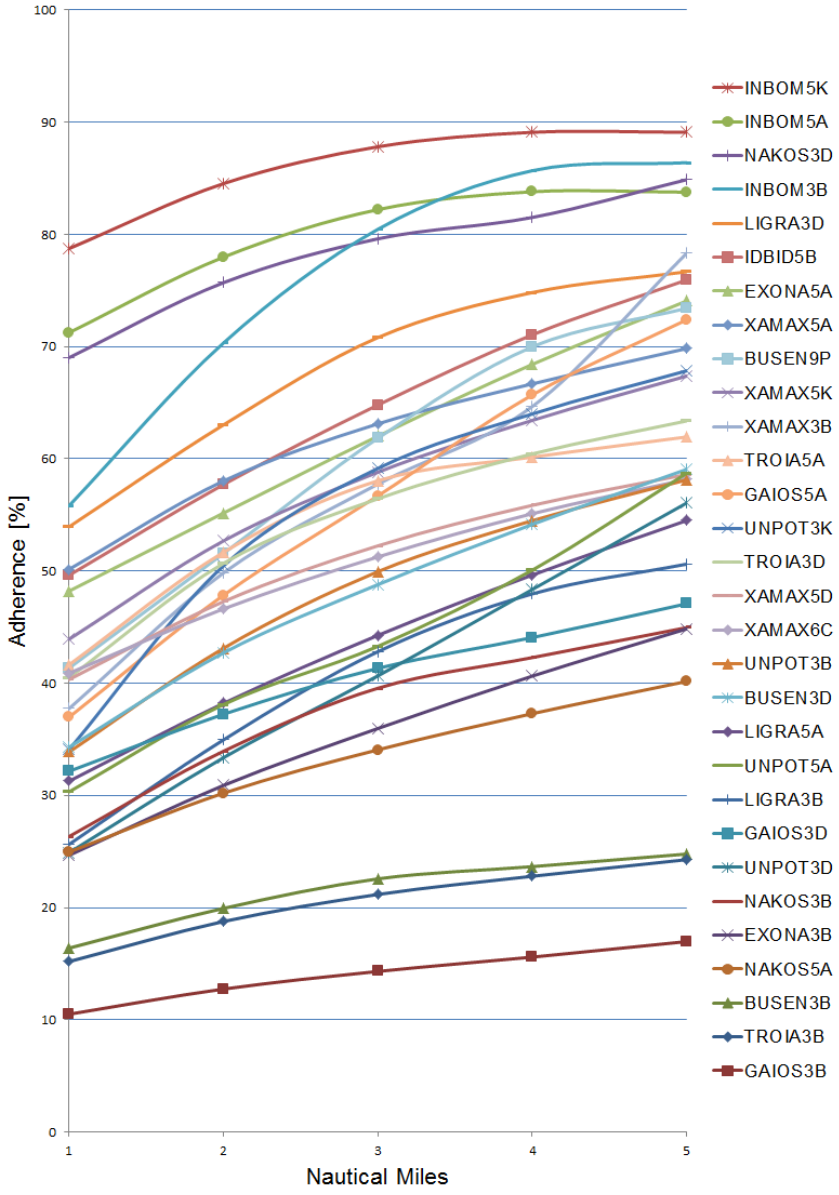

Figure 4.9: Buffer radius in nautical miles vs percentage of adherence.

4.1.5 Average STARs

With the Average STARs test 3 different patterns were produced, one for each algorithm used. Figures 4.10, 4.11 and 4.12 are 3 examples of these patterns. The one in red is the Average, in green the Weighted Average and in dark yellow the Median. The blue one is the real STAR. Not all the tracks are presented in QGIS but all of them were used in the calculations. The tracks in grey are a sample of 50 of them.

After obtaining these patterns, a comparison between each of them and the real STAR was made, i.e. the adherence for each case. The results for the 3 STARs in the images are presented in Figure 4.13.

The global results, accounting for all STARs come in Figure 4.14.

The detailed results for each pattern and every STAR come attached in Appendix A, section A.3.

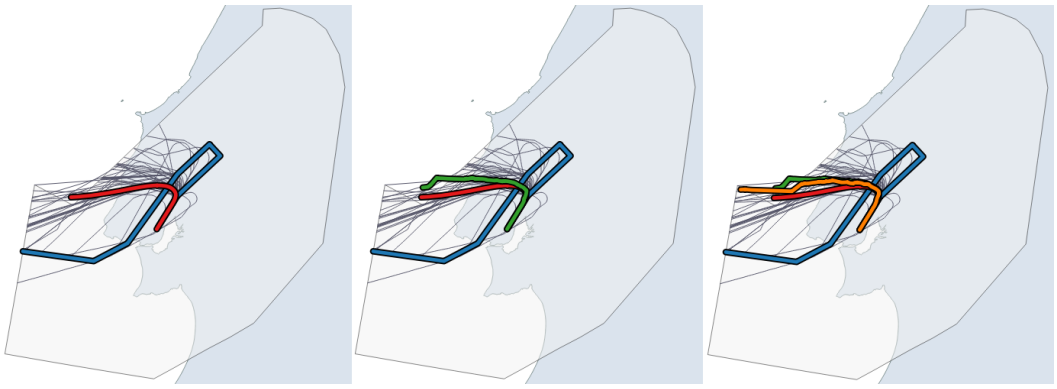

Figure 4.10: Average STARs for BUSEN3B.

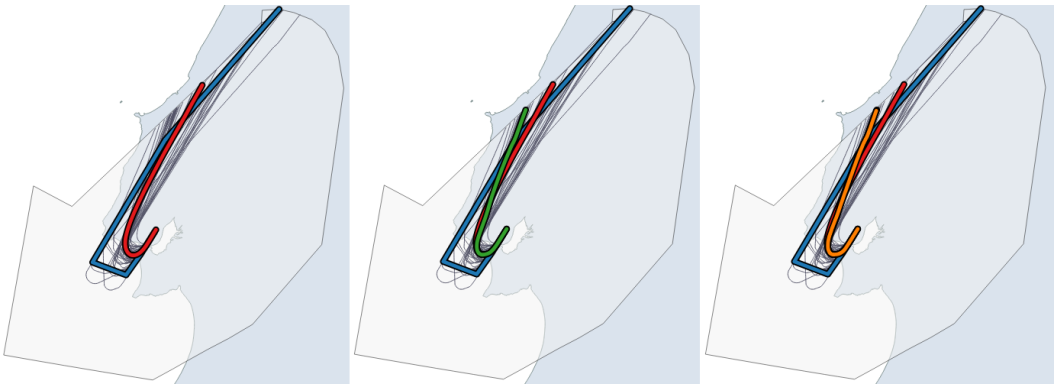

Figure 4.11: Average STARs for XAMAX6C.

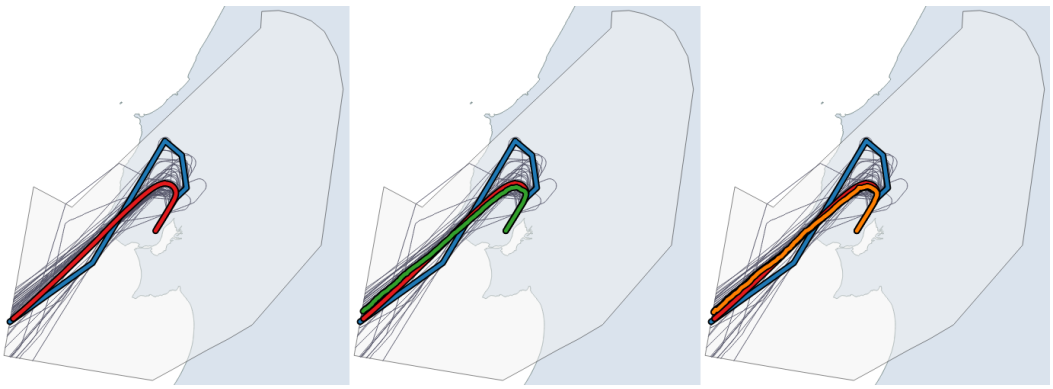

Figure 4.12: Average STARs for UNPOT3D.

	STAR	Average	Weighted Average	Median
BUSEN3B	19.56	43.90	45.88	39.61
XAMAX6C	46.03	42.79	57.64	57.21
UNPOT3D	32.84	50.76	56.50	55.91

Figure 4.13: Adherence for each pattern route for the BUSEN3B, XAMAX6C and UNPOT3D.

(a) STAR (b) Average

(c) Weighted Average (d) Median

Figure 4.14: Global Average Adherence for each pattern route.

4.1.6 Point Direct

Studying the average STARs, scenarios like the ones in Figures 4.15 and 4.16 were often found. In the images, the map on the left shows the real STAR and a sample of 50 tracks assigned to that STAR. On the right the 3 patterns obtained with the Average STARs test can be seen. For these STARs, the trajectory patterns are not best represented as lines. Here, the tracks come from a large cone shaped area of entrance and most often fly directly to a point along the STAR, closer to the runway.

Figure 4.15: Average STARs for NAKOS5A.

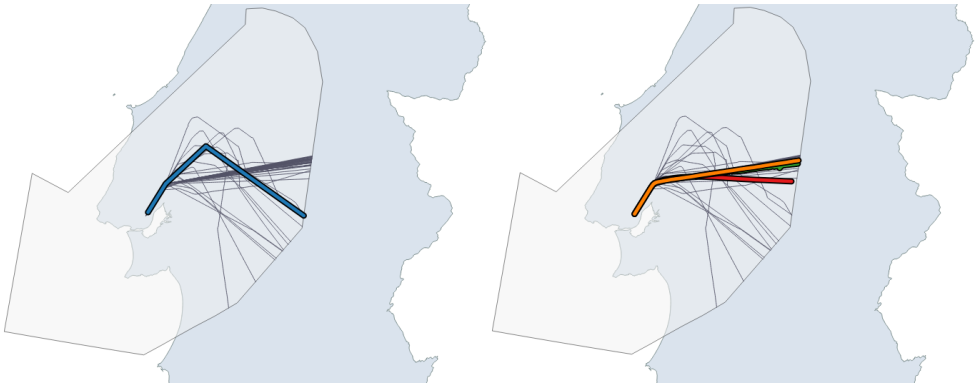

Figure 4.16: Average STARs for EXONA3B.

Because of scenarios like these, a test was made to find how many of these tracks flew directly and to what point of that STAR. The results come tabulated in Table 4.1 for the 2 STARs in the pictures: NAKOS5A and EXONA3B. In the first column comes the number of non conformative flights, i.e. flights whose adherence was less than 70%. On the second column is the number of flights that went directly

to a point along the STAR. For example, from the 771 flights in NAKOS5A, 542 of them flew directly to NETVO, which is the first point on the line of the Final Approach ILS. In Figure 4.17 the name and location of each point within the STAR can be consulted.

Flights		Direct-to			
NAKOS5A	771	NETVO: $542 = 70\%$	PT404: $47 = 6\%$	PT406: $15 = 2\%$	ADSAD: $18 = 2\%$
EXONA3B	228	UPKAT: $156 = 68\%$	PT411: $28 = 12\%$	PT410: $5 = 2\%$	RINOR: $3 = 1\%$

Table 4.1: Nonconformative flights flying directly to a STAR point.

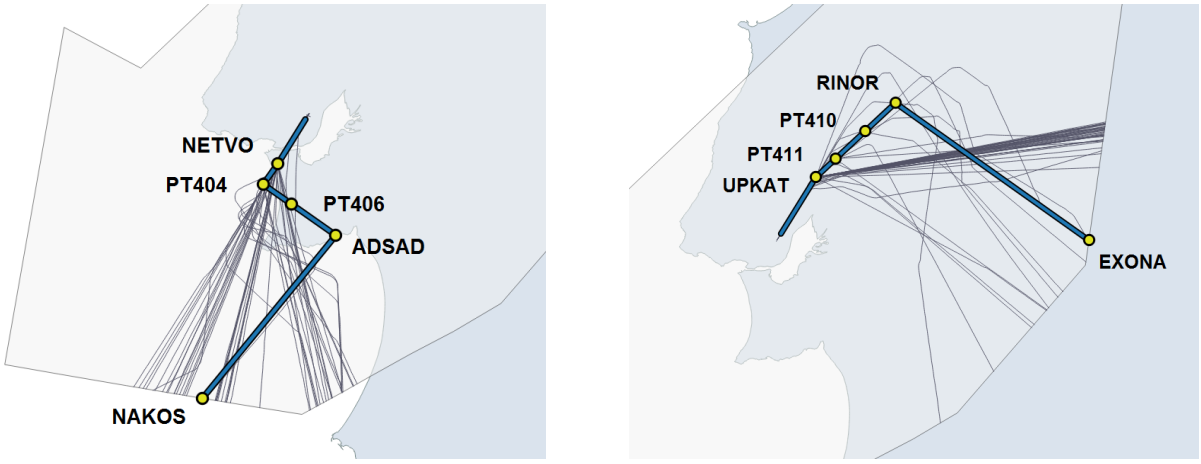

(a) NAKOS5A (b) EXONA3B

Figure 4.17: STAR points.

The complete table for all the STARs is attached in Appendix A, section A.4.

4.2 Oporto's TMA - LPPR

Oporto's airport was chosen as proof that the programs work for different locations. The parameters that needed adjustments were the definition of the TMA sector itself and the STARs. Also, the LPPT waypoint that filtered the flights to just the arrivals at Lisbon had to be substituted by LPPR.

4.2.1 3D adherence, all Data

In the 3 months, there were 4962 flights landing in Oporto, which results in an average of 54 landings per day.

Firstly, the 3D adherence regarding all data was tested. The results are illustrated in Figure 4.18.

The detailed results for each STAR come attached in Appendix A, section A.5.

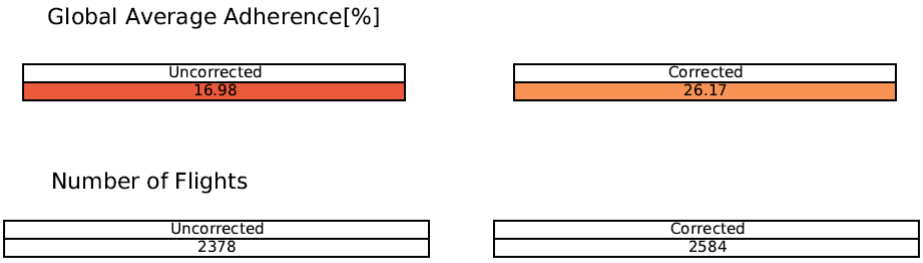

Figure 4.18: Global Average 3D Adherence for LPPR.

4.2.2 Distance Flown

As suggested by one member of the ATC at NAV, we wanted to make a test on mileage flown. For this we compared the length of the fixed paths with the length of the trajectories flown. The results come tabulated in Tables 4.2 and 4.3.

Number of Flights	Distance flown [nm]	STARs length [nm]	Mileage
4962	266879	300711	Savings of 11%

Table 4.2: Total mileage savings.

Number of Flights	Distance flown [nm]	STARs length [nm]	Mileage
4533 = 91%	238624	275355	Savings of 13%
429 = 9%	28255	25357	Spending of 11%

Table 4.3: Discriminated mileage savings and spending.

The first shows the global results and the second discriminates between aircrafts that saved and aircrafts that spent more mileage. From the 4962 flights, 91% saved mileage, i.e. if they had flown the STAR's fixed path as they were assigned to, they would have flown a bigger distance. In other words, it would have taken more time and more fuel would have been burnt.

Chapter 5

Conclusions

From this work there are multiple conclusions to be taken:

- The adhesion of a flight to its flight plan STAR is, in average, 49%. Had this information been updated during flight, the adherence would increase 10% for 29% of the flights. Regarding the segmented STAR, the increase in adherence with distance to the runway is clear. The adhesion to the first segment is, in average, 87% and the last 25%. For the corrected test these numbers increase to 89% and 34% respectively. The QGIS platform is a big advantage on this study. It gives a visual perception of the width of the buffer and where the tracks fail to adhere the most.

- The 3D adherence results are an average of 9% lower than the 2D. The tables in Figures Figure 4.5 and 4.6 show no clear relation between the segment order and the difference between 2D and 3D. Neither is there a relation between the STAR overall adherence and its difference in adherence between 2D and 3D. However, the geographical visualization of the 3D results show that this difference is notorious in the last segment: an average of 8%. Frequently the aircrafts enter the TMA at a higher altitude than the one regulated but quickly descend and return to path. On the other hand, the difference in adherences for the first segment is in average less than 1% (excluding the special case of UNPOT3K). At this stage the aircrafts are on the ILS path and don't deviate from it.

- The high vs low traffic scenario graphs show that there is no relation between the number of flights and the adherence to the STARs. Either with corrected or uncorrected data, no linear pattern could be extracted from the graphs.

- The buffer radius test led to the conclusion that a 2nm buffer was the best choice. The sequence of STARs for this buffer can be found attached in Appendix A, A.1.

- The Weighted Average and the Median provide very similar values of adherence, 66% and 67% respectively. The Average provides 62.59% of adherence, a lower value, as expected. All pattern trajectories, the Average, the Weighted Average and the Median allow for an increase in adherence, in comparison to the 58% adherence to the real STAR.

Figures 4.10, 4.11 and 4.12 show that the pattern trajectories are generally simpler and more direct shortcut versions of the real STAR. Also, the Weighted Average and the Median produce very similar lines and therefore have similar results in adherence.

- Analyzing the direct-to flights for the two examples presented in 4.1.6 it is concluded that 81% of the non conformative flights fly directly to a STAR point. The points with the biggest percentage of directs are the ones closest to the runway, i.e. the first point in line with the final approach ILS.

  In the table attached in A.4 it can be seen that this test does not apply for all the STARs. Some STARs, although having several non conformative flights, these do not fly directly to any particular point. For instance the XAMAX6C has 1380 flights, from which only 12% are directs. Besides being a small percentage it also is mainly for the two last STAR points, which makes this study not relevant for this case.

- The study for the TMA sector of Oporto shows that the corrections translate in an increase in adherence of 11%, similar to Lisbon. However, in this airport the average adherence in 3D was only of 26%, about 20% less than in Lisbon.

- Regarding distances, by not adhering to the STARs, there is an average savings of 11% of mileage flown per flight. The discriminated values show that only 9% of the flights are flying a bigger distance than they would if they were following the STAR. Considering constant speed, the relative error in time would equal the one in distance. Then, the ETA calculated by AMAN would have, in average, an error of 11% just for the TMA sector.

5.1 Achievements

Three main methodologies were developed to evaluate arrival procedures. The first one tests flight's adherence to a route. The second method traces trajectory based patterns from surveillance data. And the third one finds the incidence of direct flights and also extracts patterns from these incidences.

A set of programs to perform these methods was developed.
Regarding adherence, two programs were created to test adherence to the STARs, one for 2D and one for 3D.
A different program takes radar data and traces common trajectories forming alternative routes. Three alternative routes are obtained for each STAR, each following a different algorithm. Taking the 2D adherence test, a third adherence program was created with the distinctive option of choosing the route we are testing adherence on. This was built in order to evaluate and compare the alternative routes obtained earlier.
Another program provides, for each STAR, the percentage of direct flights to each of its STAR points.

All the tests have external programs solely for creating visual results. This includes the creation of PDF and QGIS files.
Furthermore, an additional feature of corrections was installed. It was found that some flights had better adherence results for different STARs other than the ones in their flight plan. For this reason, all the programs either present results for both STARs (corrected or uncorrected) or have the option to choose wether to test corrected or uncorrected data.

Several results were taken from the programs. We quantified 2D and 3D adherence and, by comparison, were able to find where the 3D was lacking. A relation between amount of traffic and adherence was sought. The best buffer radius to use in the different tests was found. The alternative routes were extracted for every STAR and their adherences were compared among them and with the raw STAR. Direct flight's incidence for each STAR and each STAR point was found.
The programs were tested for two different airports as proof of generality. The 3D adherence was tested for the second airport and compared between the two. Lastly, a test was made on distance flown, spendings and savings.

This work has already triggered some discussion among workers at NAV Portugal.

Members of the ATC team showed great appreciation for it. Techniques such as vectoring, change in STARs and granting direct flights are daily practices. Still, the way this information is now available is a valuable asset on traffic flow's analysis. Moreover it is a refreshing view on these practices.

I have personally attended the first meeting between the development team and the ATCOs at NAV to demonstrate some of the results and start a discussion on the topic. These meetings are to be continued and hopefully this work will assist and expedite the process of designing the optimal solution for the TMA sector in Lisbon.

5.2 Recommendations

For AMAN to be ready to be fully integrated into the system, the latter needs some improvements. A personal suggestion would be to undertake Point Merge and reduce the number of merging points to a minimum.

A final test was conducted for Lisbon's TMA to support the Point Merge undertake. The STARs were divided in 4 groups according to their assigned RWY and origin: North or South of the TMA. All the Median routes obtained with the Average STARs program were gathered and divided into the same groups.

The STARs and respective Median routes from these 4 groups are shown on Figures 5.1, 5.2, 5.3 and 5.4. On the left are the STARs, in blue, and on the right the Median routes in dark yellow.

Figure 5.1 shows that the way these STARs are structured already indicates two stand out merging points: EKMAR and ADSAD. The Median routes, traced from real trajectories, confirm that there is already a tendency to merge the flights. Not only that, but also there is a tendency to further direct the flight into just one merging point: NETVO.

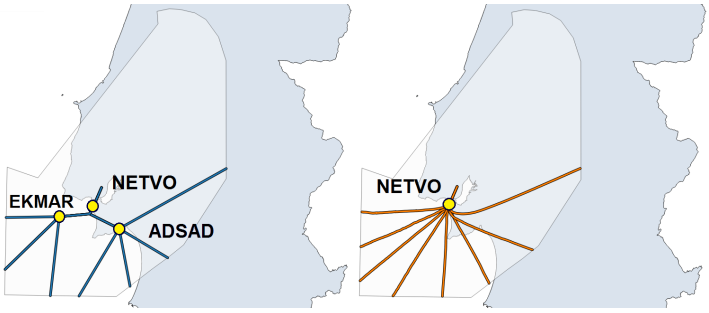

Figure 5.1: STARs and respective Median routes for RWYs 3/35, from the South.

Similarly to 5.1, Figures 5.2 and 5.3 also show promising merging points in the STAR structure on the left but one clear stand out effective point on the right.

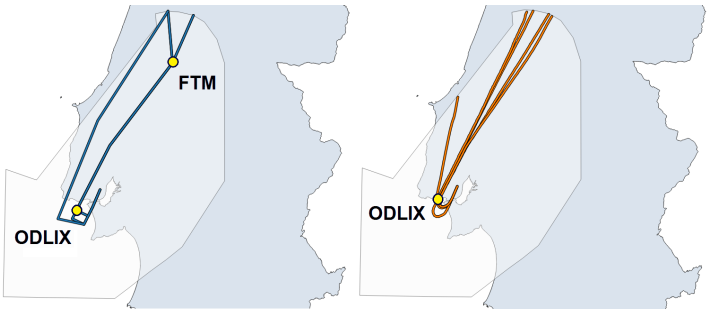

Figure 5.2: STARs and respective Median routes for RWYs 3/35, from the North.

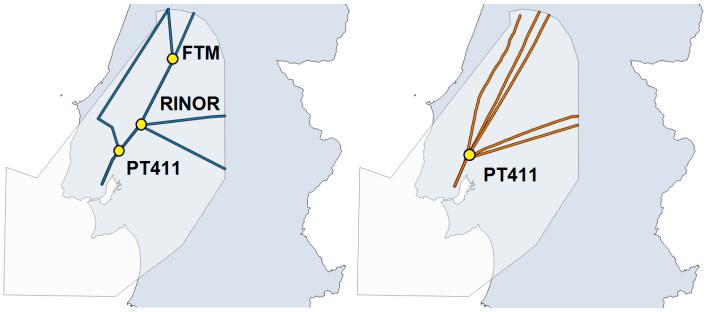

Figure 5.3: STARs and respective Median routes for RWY 21, from the North.

Lastly, the STARs originating from the South and destined to RWY 21, represented on Figure 5.4, were subdivided into STARs that ended in 3B and 3D for a clearest presentation. Both STAR's structures point to the same merging point: EKMAR. However this is not the case for the Median routes, neither is there another clear merging point. Still, PT405 stands out for the trajectories turning East for landing.

Lisbon's TMA has every visible condition to proceed with Point Merge. Not only do STAR's paths

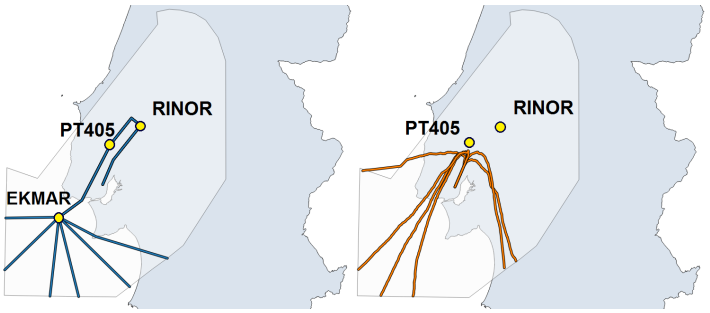

(a) 3B

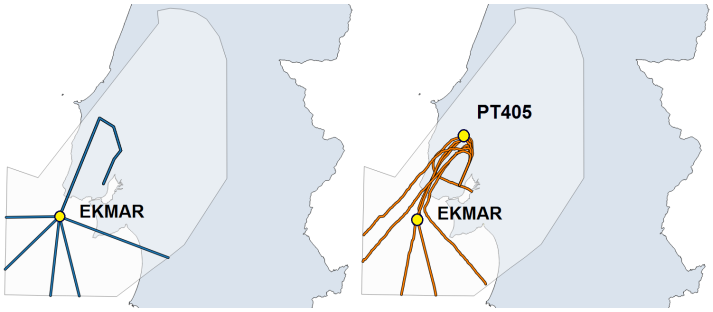

(b) 3D

Figure 5.4: STARs and respective Median routes for RWY 21, from the South.

already indicate merging points but also the median proves that aircrafts do in fact merge into points. Furthermore, figures 5.1, 5.2 and 5.3 show that merging points can be reduced and paths can be simplified.

5.3 Future Work

A proposal for future work would be to downsize the minimum scale of results, i.e. instead of the minimum being one day, make it hours or smaller time periods like morning, afternoon and evening. That would give us an idea of how the slots are distributed throughout the day and a relation between number of flights and adherence could then be extracted.

A second proposal would be the development of methods and algorithms capable of infering alternative STARs through 3D surveillance data.

Presenting results for every airport in Portugal would possibly initiate the idea of a TMA restructuring nation wise.

Lastly, and for the reasons presented in Recommendations, a future development on the Point Merge study is suggested.

Bibliography

[1] *Local Single Sky ImPlementation (LSSIP) Portugal, Year 2014 - Level 1*. EUROCONTROL Agency. URL http://www.eurocontrol.int/sites/default/files/content/documents/official-documents/reports/lssip2014-portugal.pdf.

[2] Lisbon's FIR Traffic Evolution in June 2015. URL http://www.nav.pt/Ficheiros/Mov_RIVLIS_Jun15.pdf.

[3] N. Hasevoets and P. Conroy. *AMAN Implementation GUIDELINES*. EUROCONTROL Agency, 0.1 edition, December 2010. URL https://www.eurocontrol.int/sites/default/files/article/content/documents/nm/fasti-aman-guidelines-2010.pdf.

[4] eAIP Portugal. Technical report, NAV Portugal, 2015.

[5] T. D. N. F. Nga Bui, Caroline Chabrol and J. Vannier. *Step 1 AMAN + Point Merge in E-TMA - SPR*, 00.01.01 edition, April 2013. URL http://www.sesarju.eu/sesar-solutions/traffic-synchronisation/arrival-management-aman-and-point-merge.

[6] Innovative Flight Procedures. URL http://www.flugl\unhbox\voidb@x\bgroup\accent127a\penalty\@M\hskip\z@skip\egrouprm-portal.de/laerm-vermeiden/innovative-flugverfahren. Last consulted 2015/09/16.

[7] IAA. IAA's award-winning innovation saved airlines €5.5m in 2013. *Air Transport News*, December 2013. URL http://www.atn.aero/article.pl?categ=&id=47038#.

[8] S. J. Zelinski and J. Jung. Arrival scheduling with shortcut path options and mixed aircraft performance. Presented at the Tenth USA/Europe ATM Research and Development Seminar (ATM 2015), June 2015. URL http://www.atmseminar.org/seminarContent/seminar11/papers/415_Zelinski_0126151019-Final-Paper-4-29-15.pdf.

[9] S. Gillies. *The Shapely User Manual*, 1.2 and 1.3 edition, December 2013. URL http://toblerity.org/shapely/manual.html.

Appendix A

Appendix A

A.1 2D Adherence, all Flights

All_Flights 2NM Buffer

Flight Plan Information only

	Adherence[%]
GAIOS3B	13.09
TROIA3B	16.63
BUSEN3B	22.32
XAMAX6C	25.11
UNPOT3B	25.49
NAKOS5A	28.42
NAKOS3B	29.09
LIGRA3B	31.53
EXONA3B	31.70
XAMAX5D	32.40
UNPOT5A	37.54
LIGRA5A	38.39
TROIA5A	45.97
GAIOS5A	47.76
IDBID5B	48.31
BUSEN9P	50.45
EXONA5A	55.03
INBOM3B	65.46
INBOM5A	74.58

	Number of Flights
GAIOS3B	47
TROIA3B	146
BUSEN3B	173
XAMAX6C	4035
UNPOT3B	127
NAKOS5A	656
NAKOS3B	127
LIGRA3B	59
EXONA3B	55
XAMAX5D	1039
UNPOT5A	572
LIGRA5A	354
TROIA5A	621
GAIOS5A	379
IDBID5B	800
BUSEN9P	696
EXONA5A	3429
INBOM3B	1177
INBOM5A	4468
Total	18960

	1	2	3	4	5	6	7	8	9	10	11	12
GAIOS3B	89.63	65.92	19.71	10.07	4.27	1.06	2.69	0.34	0.00	0.00	0.00	1.12
TROIA3B	88.14	60.84	18.88	2.45	0.49	1.09	4.05	6.12	5.53	3.66		
BUSEN3B	89.28	51.57	6.38	0.54	0.32	4.90	13.80	11.99	7.52	17.57		
XAMAX6C	84.97	61.11	20.93	8.62	2.70	18.99	18.34					
UNPOT3B	87.10	47.24	5.84	1.72	1.30	3.19	12.88	16.18	13.77	25.39		
NAKOS5A	89.34	85.64	36.86	1.19	9.07							
NAKOS3B	84.51	53.53	6.95	2.24	1.27	1.90	10.80	37.78	20.78	18.85		
LIGRA3B	90.93	54.96	10.92	3.01	0.00	2.08	8.98	32.23	33.54	22.67		
EXONA3B	88.67	64.85	29.89	15.93	11.92							
XAMAX5D	90.52	75.71	35.41	9.53	16.06							
UNPOT5A	85.29	74.94	37.64	14.93								
LIGRA5A	90.33	90.62	22.77	21.84								
TROIA5A	84.10	56.56	40.85	24.36	5.22							
GAIOS5A	84.56	58.47	35.79	42.77	32.17							
IDBID5B	88.66	71.72	27.47	21.99	34.83	43.07						
BUSEN9P	86.32	63.32	35.18	38.23								
EXONA5A	83.86	59.19	35.69	25.68	53.27							
INBOM3B	90.91	83.00	64.40	42.39	54.78	52.72						
INBOM5A	84.73	59.60	20.17	12.18	23.87	59.38	87.52	81.86	63.79			

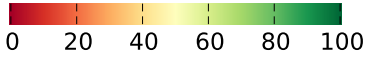

All_Flights 2NM Buffer

Infered ATC intervention on STAR attribution

	Adherence[%]
GAIOS3B	12.75
TROIA3B	18.77
BUSEN3B	19.94
NAKOS5A	30.21
EXONA3B	30.90
UNPOT3D	33.37
NAKOS3B	33.95
LIGRA3B	34.96
GAIOS3D	37.24
UNPOT5A	38.11
LIGRA5A	38.22
BUSEN3D	42.71
UNPOT3B	43.12
XAMAX6C	46.63
XAMAX5D	47.28
GAIOS5A	47.85
XAMAX3B	49.84
UNPOT3K	50.47
TROIA3D	50.69
BUSEN9P	51.57
TROIA5A	51.68
XAMAX5K	52.69
EXONA5A	55.17
IDBID5B	57.71
XAMAX5A	58.03
LIGRA3D	63.03
INBOM3B	70.33
NAKOS3D	75.70
INBOM5A	77.98
INBOM5K	84.53

	Number of Flights
GAIOS3B	97
TROIA3B	90
BUSEN3B	131
NAKOS5A	778
EXONA3B	235
UNPOT3D	57
NAKOS3B	82
LIGRA3B	46
GAIOS3D	14
UNPOT5A	554
LIGRA5A	548
BUSEN3D	74
UNPOT3B	42
XAMAX6C	1947
XAMAX5D	587
GAIOS5A	407
XAMAX3B	182
UNPOT3K	73
TROIA3D	3
BUSEN9P	643
TROIA5A	312
XAMAX5K	825
EXONA5A	3440
IDBID5B	605
XAMAX5A	157
LIGRA3D	11
INBOM3B	1429
NAKOS3D	12
INBOM5A	4452
INBOM5K	1127
Total	18960

	1	2	3	4	5	6	7	8	9	10	11	12
GAIOS3B	87.68	52.08	9.80	3.97	1.61	0.14	0.73	0.16	0.00	0.00	0.00	6.82
TROIA3B	91.49	71.31	30.40	4.24	0.80	2.18	2.70	8.71	5.15	3.08		
BUSEN3B	90.60	46.74	5.20	0.72	0.34	3.15	9.36	14.82	6.22	8.61		
NAKOS5A	86.16	73.97	37.88	5.24	12.13							
EXONA3B	89.69	63.18	12.70	6.28	14.82							
UNPOT3D	89.37	43.70	15.47	5.28	29.56	18.92	21.24					
NAKOS3B	90.95	61.30	9.34	3.47	1.97	1.43	11.02	56.38	23.73	15.24		
LIGRA3B	93.14	56.61	11.66	3.86	0.00	2.49	8.49	38.25	40.09	25.31		
GAIOS3D	91.43	50.93	6.95	2.54	49.86	26.17	20.92					
UNPOT5A	85.78	75.39	38.35	15.34								
LIGRA5A	90.51	91.55	21.95	21.86								
BUSEN3D	91.76	60.06	33.38	26.25	32.29	8.86	31.98					
UNPOT3B	95.41	60.98	13.07	5.19	3.94	4.65	16.32	25.20	37.84	61.05		
XAMAX6C	86.61	68.55	29.03	15.00	6.49	45.81	43.62					
XAMAX5D	92.46	68.65	41.77	23.20	36.35							
GAIOS5A	84.92	59.57	35.64	41.48	32.66							
XAMAX3B	91.79	83.43	50.97	20.08	27.70	42.87						
UNPOT3K	85.59	66.90	57.24	27.85								
TROIA3D	92.14	59.25	55.66	60.54	67.02	17.71	8.12					
BUSEN9P	86.44	63.15	33.09	41.94								
TROIA5A	86.37	54.04	45.37	37.83	8.21							
XAMAX5K	83.22	47.99	29.07	51.86	92.08	30.58	31.96					
EXONA5A	83.94	59.09	35.56	25.74	53.46							
IDBID5B	91.20	76.91	33.91	27.96	46.19	57.33						
XAMAX5A	89.85	88.42	59.24	47.56	69.26	87.73	92.23	31.97	30.96			
LIGRA3D	91.99	61.13	18.13	9.31	65.13	59.27	65.93					
INBOM3B	92.25	86.00	69.72	44.06	58.65	60.96						
NAKOS3D	92.18	64.11	51.63	29.05	74.15	64.59	78.50					
INBOM5A	84.93	60.15	21.49	13.85	26.01	62.26	91.62	86.00	67.43			
INBOM5K	84.06	53.98	37.24	58.27	92.66	85.74	78.58					

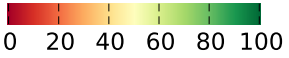

A.2 3D Corrected Adherence, all Flights

All_Flights 2NM Buffer

Infered ATC intervention on STAR attribution

	Adherence[%]
UNPOT3K	12.17
GAIOS3B	12.18
BUSEN3B	16.25
TROIA3B	17.37
XAMAX5K	21.89
NAKOS3B	26.42
LIGRA3B	28.93
NAKOS5A	30.09
EXONA3B	30.37
UNPOT3D	31.00
INBOM5K	32.42
GAIOS3D	34.84
UNPOT5A	37.27
UNPOT3B	37.65
LIGRA5A	37.96
BUSEN3D	38.72
XAMAX6C	43.04
TROIA3D	43.76
XAMAX5D	44.51
GAIOS5A	47.38
XAMAX3B	49.23
BUSEN9P	50.62
TROIA5A	51.18
XAMAX5A	53.04
EXONA5A	53.49
IDBID5B	53.72
LIGRA3D	59.12
INBOM5A	64.36
NAKOS3D	67.94
INBOM3B	68.57

	Number of Flights
UNPOT3K	73
GAIOS3B	97
BUSEN3B	131
TROIA3B	90
XAMAX5K	825
NAKOS3B	82
LIGRA3B	46
NAKOS5A	778
EXONA3B	235
UNPOT3D	57
INBOM5K	1127
GAIOS3D	14
UNPOT5A	554
UNPOT3B	42
LIGRA5A	548
BUSEN3D	74
XAMAX6C	1947
TROIA3D	3
XAMAX5D	587
GAIOS5A	407
XAMAX3B	182
BUSEN9P	643
TROIA5A	312
XAMAX5A	157
EXONA5A	3440
IDBID5B	605
LIGRA3D	11
INBOM5A	4451
NAKOS3D	12
INBOM3B	1429
Total	18959

	1	2	3	4	5	6	7	8	9	10	11	12
UNPOT3K	0.12	34.57	18.26	4.90								
GAIOS3B	86.28	35.46	9.80	3.97	1.61	0.14	0.42	0.00	0.00	0.00	0.00	6.58
BUSEN3B	89.16	36.97	5.20	0.72	0.28	1.50	3.00	3.40	6.09	8.14		
TROIA3B	90.75	63.41	30.34	2.60	0.48	1.48	0.06	5.11	5.10	2.96		
XAMAX5K	78.52	37.23	9.21	5.22	23.49	16.77	0.75					
NAKOS3B	90.14	52.35	9.34	2.72	0.80	1.07	3.12	28.12	23.27	14.93		
LIGRA3B	90.70	46.24	11.66	3.82	0.00	2.49	3.03	16.27	40.09	25.08		
NAKOS5A	86.10	68.04	35.70	5.07	11.97							
EXONA3B	89.43	58.22	12.70	5.49	14.45							
UNPOT3D	89.00	38.48	6.48	3.01	27.41	18.92	20.17					
INBOM5K	79.93	42.75	13.48	7.88	27.17	39.15	0.77					
GAIOS3D	91.44	40.71	0.00	2.31	44.98	26.17	20.92					
UNPOT5A	85.57	69.07	38.18	14.28								
UNPOT3B	91.38	57.11	13.07	4.07	1.89	1.86	4.13	13.75	35.66	57.22		
LIGRA5A	90.21	85.07	21.47	21.83								
BUSEN3D	91.44	55.93	15.97	19.15	30.02	8.86	29.97					
XAMAX6C	86.45	60.94	28.96	14.89	5.42	41.20	39.27					
TROIA3D	92.14	55.48	0.00	35.80	65.21	17.71	8.12					
XAMAX5D	92.22	65.92	30.38	19.54	34.66							
GAIOS5A	84.62	50.20	34.13	41.02	32.18							
XAMAX3B	91.77	80.99	50.91	19.85	27.53	41.25						
BUSEN9P	86.13	54.19	32.73	40.81								
TROIA5A	86.07	47.05	44.83	37.36	7.54							
XAMAX5A	89.68	81.52	59.24	47.02	68.39	87.20	90.74	28.47	12.73			
EXONA5A	83.75	51.82	34.46	25.60	51.19							
IDBID5B	91.01	74.01	33.90	27.30	42.33	40.99						
LIGRA3D	91.99	55.01	3.84	4.08	60.47	59.27	65.93					
INBOM5A	84.68	52.71	21.43	13.63	25.66	58.35	82.42	75.61	24.58			
NAKOS3D	90.77	55.14	20.00	19.89	65.66	60.02	76.32					
INBOM3B	92.08	83.38	69.72	42.98	57.92	56.38						

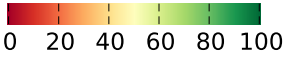

A.3 Average STARs

All Flights STAR 2NM Buffer

Infered ATC intervention

	Adherence[%]
GAIOS3B	12.52
TROIA3B	18.37
BUSEN3B	19.56
NAKOS5A	29.50
EXONA3B	30.41
UNPOT3D	32.84
NAKOS3B	33.34
LIGRA3B	34.32
GAIOS3D	36.59
UNPOT5A	37.30
LIGRA5A	37.35
BUSEN3D	41.99
UNPOT3B	42.42
XAMAX6C	46.03
XAMAX5D	46.66
GAIOS5A	46.73
XAMAX3B	48.86
UNPOT3K	49.68
TROIA3D	49.96
TROIA5A	50.11
BUSEN9P	50.72
XAMAX5K	51.70
EXONA5A	54.53
IDBID5B	56.43
XAMAX5A	56.49
LIGRA3D	62.03
INBOM3B	68.92
NAKOS3D	74.41
INBOM5A	76.70
INBOM5K	83.18

	Number of Flights
GAIOS3B	97
TROIA3B	90
BUSEN3B	131
NAKOS5A	778
EXONA3B	235
UNPOT3D	57
NAKOS3B	82
LIGRA3B	46
GAIOS3D	14
UNPOT5A	554
LIGRA5A	548
BUSEN3D	74
UNPOT3B	42
XAMAX6C	1947
XAMAX5D	587
GAIOS5A	407
XAMAX3B	182
UNPOT3K	73
TROIA3D	3
TROIA5A	312
BUSEN9P	643
XAMAX5K	825
EXONA5A	3440
IDBID5B	605
XAMAX5A	157
LIGRA3D	11
INBOM3B	1429
NAKOS3D	12
INBOM5A	4452
INBOM5K	1127
Total	18960

Global Average Adherence [%]
57.69

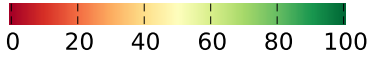

All Flights Average 2NM Buffer

Infered ATC intervention

	Adherence[%]
GAIOS3D	22.43
NAKOS3B	27.07
GAIOS3B	30.64
TROIA3B	32.76
BUSEN3D	34.45
LIGRA3B	34.92
UNPOT3B	38.69
TROIA3D	40.96
NAKOS5A	42.26
XAMAX6C	42.79
BUSEN3B	43.90
XAMAX5D	44.49
EXONA3B	48.81
UNPOT3D	50.76
BUSEN9P	51.23
IDBID5B	53.38
GAIOS5A	55.30
EXONA5A	58.79
TROIA5A	62.68
INBOM3B	64.33
LIGRA3D	69.71
LIGRA5A	69.88
XAMAX3B	70.24
XAMAX5A	71.57
NAKOS3D	73.16
UNPOT5A	73.63
INBOM5K	74.62
UNPOT3K	75.98
XAMAX5K	76.34
INBOM5A	78.85

	Number of Flights
GAIOS3D	14
NAKOS3B	82
GAIOS3B	97
TROIA3B	90
BUSEN3D	74
LIGRA3B	46
UNPOT3B	42
TROIA3D	3
NAKOS5A	778
XAMAX6C	1947
BUSEN3B	131
XAMAX5D	587
EXONA3B	235
UNPOT3D	57
BUSEN9P	643
IDBID5B	605
GAIOS5A	407
EXONA5A	3440
TROIA5A	312
INBOM3B	1429
LIGRA3D	11
LIGRA5A	548
XAMAX3B	182
XAMAX5A	157
NAKOS3D	12
UNPOT5A	554
INBOM5K	1127
UNPOT3K	73
XAMAX5K	825
INBOM5A	4452
Total	18960

Global Average Adherence [%]
62.59

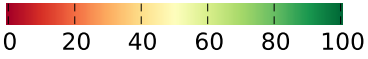

All Flights Weighted_Average 2NM Buffer

Infered ATC intervention

	Adherence[%]
GAIOS3B	28.47
GAIOS3D	30.68
TROIA3B	33.26
BUSEN3D	34.06
XAMAX5D	34.92
TROIA3D	40.96
LIGRA3B	42.21
BUSEN3B	45.88
NAKOS5A	47.36
NAKOS3B	48.26
BUSEN9P	48.31
UNPOT3D	56.50
EXONA5A	56.51
GAIOS5A	56.83
UNPOT3B	57.14
XAMAX6C	57.64
IDBID5B	58.60
TROIA5A	63.13
LIGRA3D	69.26
LIGRA5A	69.93
XAMAX3B	70.43
EXONA3B	70.99
XAMAX5A	71.25
INBOM5K	72.16
NAKOS3D	72.47
INBOM3B	74.20
UNPOT3K	74.99
UNPOT5A	75.21
XAMAX5K	76.25
INBOM5A	85.64

	Number of Flights
GAIOS3B	97
GAIOS3D	14
TROIA3B	90
BUSEN3D	74
XAMAX5D	587
TROIA3D	3
LIGRA3B	46
BUSEN3B	131
NAKOS5A	778
NAKOS3B	82
BUSEN9P	643
UNPOT3D	57
EXONA5A	3440
GAIOS5A	407
UNPOT3B	42
XAMAX6C	1947
IDBID5B	605
TROIA5A	312
LIGRA3D	11
LIGRA5A	548
XAMAX3B	182
EXONA3B	235
XAMAX5A	157
INBOM5K	1127
NAKOS3D	12
INBOM3B	1429
UNPOT3K	73
UNPOT5A	554
XAMAX5K	825
INBOM5A	4452
Total	18960

Global Average Adherence [%]
66.40

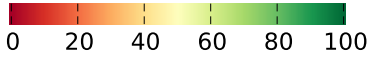

All Flights Median 2NM Buffer

Infered ATC intervention

	Adherence[%]
GAIOS3B	31.75
BUSEN3D	32.34
TROIA3B	34.08
XAMAX5D	37.41
GAIOS3D	38.50
BUSEN3B	39.61
TROIA3D	40.96
LIGRA3B	44.94
BUSEN9P	48.34
NAKOS5A	48.83
NAKOS3B	48.98
UNPOT3D	55.91
GAIOS5A	56.52
UNPOT3B	56.54
EXONA5A	56.55
XAMAX6C	57.21
IDBID5B	58.31
TROIA5A	62.64
LIGRA5A	69.76
XAMAX3B	70.43
LIGRA3D	70.85
XAMAX5A	71.14
INBOM5K	72.76
NAKOS3D	73.66
EXONA3B	73.92
INBOM3B	74.20
UNPOT3K	74.97
UNPOT5A	75.01
XAMAX5K	76.26
INBOM5A	86.21

	Number of Flights
GAIOS3B	97
BUSEN3D	74
TROIA3B	90
XAMAX5D	587
GAIOS3D	14
BUSEN3B	131
TROIA3D	3
LIGRA3B	46
BUSEN9P	643
NAKOS5A	778
NAKOS3B	82
UNPOT3D	57
GAIOS5A	407
UNPOT3B	42
EXONA5A	3440
XAMAX6C	1947
IDBID5B	605
TROIA5A	312
LIGRA5A	548
XAMAX3B	182
LIGRA3D	11
XAMAX5A	157
INBOM5K	1127
NAKOS3D	12
EXONA3B	235
INBOM3B	1429
UNPOT3K	73
UNPOT5A	554
XAMAX5K	825
INBOM5A	4452
Total	18960

Global Average Adherence [%]
66.66

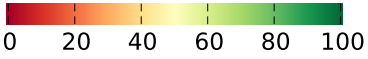

A.4 Point Direct

	Flights	Direct-to
BUSEN3B	129	UPKAT: 11, PT411: 2, PT408: 1, PT407: 1, PT405: 45, ODLIX: 3, EKMAR: 2
BUSEN3D	61	PT411: 1, PT415: 7, UMUPI: 4, PT414: 1
BUSEN9P	468	NETVO: 231, PT404: 79, EKMAR: 54, BUSEN: 1
EXONA3B	228	UPKAT: 156, PT411: 28, PT410: 5, RINOR: 3
EXONA5A	2064	NETVO: 27, PT404: 60, PT406: 577, ADSAD: 51
GAIOS3B	97	UPKAT: 2, PT411: 31, PT410: 1, RINOR: 4
GAIOS3D	14	PT411: 1, PT414: 10
GAIOS5A	352	NETVO: 79, PT404: 79, PT406: 69, ADSAD: 43
IDBID5B	399	UPKAT: 153, PT411: 57, PT410: 13, RINOR: 9
INBOM3B	699	UPKAT: 500, PT411: 7, PT410: 8, RINOR: 9, FTM: 63
INBOM5A	1160	NETVO: 3, PT403: 2, PT402: 9, PT401: 26, ODLIX: 35, PT405: 778, FTM: 134
INBOM5K	238	NETVO: 2, PT404: 1, PT401: 10, ODLIX: 49, PT405: 114, FTM: 17
LIGRA3B	46	UPKAT: 1, PT407: 2, PT405: 11, ODLIX: 10, EKMAR: 9
LIGRA3D	9	UMUPI: 1, PT414: 6
LIGRA5A	539	NETVO: 482, PT404: 7, EKMAR: 2
NAKOS3B	81	PT410: 1, PT405: 10, ODLIX: 32, EKMAR: 2
NAKOS3D	4	PT414: 3
NAKOS5A	771	NETVO: 542, PT404: 47, PT406: 15, ADSAD: 18
TROIA3B	90	PT411: 4, PT410: 3, RINOR: 2, ODLIX: 1, EKMAR: 2, TROIA: 8
TROIA5A	285	NETVO: 201, PT404: 23, PT406: 12, ADSAD: 17
UNPOT3B	38	PT410: 1, PT405: 5, ODLIX: 8, EKMAR: 5
UNPOT3D	55	PT415: 5, UMUPI: 1, PT414: 14
UNPOT3K	73	NETVO: 52, PT404: 6, EKMAR: 4
UNPOT5A	513	NETVO: 425, PT404: 21, EKMAR: 1
XAMAX3B	134	UPKAT: 99, PT411: 1, RINOR: 3, FTM: 7
XAMAX5A	129	PT402: 95, PT401: 3, ODLIX: 2, PT405: 18
XAMAX5D	444	UPKAT: 217, PT411: 9, PT415: 4, UMUPI: 33
XAMAX5K	703	PT401: 379, ODLIX: 242, PT405: 30, FTM: 11
XAMAX6C	1380	NETVO: 2, PT404: 1, PT403: 2, EKMAR: 83, UMUPI: 77

Table A.1: Direct-to points tabled data.

A.5 Oporto's TMA - LPPR

All_Flights 2NM Buffer

Global Average Adherence[%]

Uncorrected	Corrected
16.98	26.17

Number of Flights

Uncorrected	Corrected
2378	2584

	Uncorrected	ASPOR9T	ELGIX9T	PESUL1T	MALIS2C	INKIT3C	ASPOR3A	ABLEG9M	MALIS2T	LAVPA9M	ASPOR3C	TOVBA9M	PESUL3C	LAVPA3A	TURON3A	ABLEG3C	ABLEG9T	TURON9T
ASPOR9T	0	0	0	0	0	2	0	0	0	0	0	0	0	0	0	0	0	0
ABLEG9T	11	0	0	0	0	0	0	150	0	9	0	1	0	99	1	325	0	0
ELGIX9T	457	0	0	20	2	419	0	1	4	0	1	0	25	0	0	1	0	0
LAVPA9M	46	0	0	0	0	0	0	0	0	0	0	0	0	106	0	0	0	0
TOVBA9M	13	0	0	0	0	0	0	0	0	2	0	0	0	12	0	0	0	0
INKIT3C	1241	0	217	1	7	0	1	0	2	0	0	0	14	0	0	1	0	0
PESUL3C	209	0	38	195	0	523	0	0	0	0	1	0	0	3	0	2	1	0
LAVPA3A	128	1	0	0	0	0	0	0	0	36	0	15	0	0	0	0	0	1
ABLEG3C	270	0	0	0	0	0	0	133	0	21	0	0	0	180	2	0	9	0
MALIS2C	2	0	0	0	0	0	0	0	0	0	0	0	0	0	0	0	0	0
ASPOR3C	1	0	0	0	0	0	0	0	0	0	0	0	0	0	0	0	0	0

All_Flights 2NM Buffer

Flight Plan Information only

	Adherence[%]
ASPOR9T	1.21
ABLEG9T	4.50
ELGIX9T	8.28
LAVPA9M	11.24
TOVBA9M	18.30
INKIT3C	19.84
PESUL3C	20.99
LAVPA3A	26.92
ABLEG3C	27.41
MALIS2C	35.36
ASPOR3C	41.84

	Number of Flights
ASPOR9T	2
ABLEG9T	596
ELGIX9T	930
LAVPA9M	152
TOVBA9M	27
INKIT3C	1484
PESUL3C	972
LAVPA3A	181
ABLEG3C	615
MALIS2C	2
ASPOR3C	1
Total	4962

	1	2	3	4	5	6	7	8
ASPOR9T	8.24	0.00	0.00	0.00	0.00	0.00		
ABLEG9T	19.94	10.66	9.96	0.54	0.56	1.08	0.81	0.59
ELGIX9T	28.65	20.19	17.23	3.21	2.82	1.45	3.18	
LAVPA9M	18.50	9.46	8.36	1.48	10.70			
TOVBA9M	26.21	20.73	23.04	4.87	9.02			
INKIT3C	66.38	22.11	2.59	1.43	0.44	9.09		
PESUL3C	63.62	25.31	4.09	2.85	2.49			
LAVPA3A	58.51	20.75	12.82	16.51				
ABLEG3C	67.20	50.78	4.42	0.67				
MALIS2C	86.72	80.67	78.05	65.29	42.65	10.54		
ASPOR3C	135.57	155.96	83.59	7.69	0.00	0.00	0.00	0.00

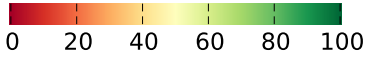

All_Flights 2NM Buffer

Infered ATC intervention on STAR attribution

	Adherence[%]
ASPOR9T	11.89
ELGIX9T	14.37
PESUL1T	15.93
MALIS2C	19.21
INKIT3C	24.15
ASPOR3A	25.08
ABLEG9M	25.15
MALIS2T	27.97
LAVPA9M	30.98
ASPOR3C	31.01
TOVBA9M	32.70
PESUL3C	34.68
LAVPA3A	35.91
TURON3A	37.42
ABLEG3C	37.96
ABLEG9T	39.58
TURON9T	43.48

	Number of Flights
ASPOR9T	1
ELGIX9T	712
PESUL1T	216
MALIS2C	11
INKIT3C	2185
ASPOR3A	1
ABLEG9M	284
MALIS2T	6
LAVPA9M	114
ASPOR3C	3
TOVBA9M	29
PESUL3C	248
LAVPA3A	528
TURON3A	3
ABLEG3C	599
ABLEG9T	21
TURON9T	1
Total	4962

	1	2	3	4	5	6	7	8	9
ASPOR9T	42.25	35.55	35.35	0.00	0.00	0.00			
ELGIX9T	46.40	37.95	32.20	5.77	4.62	2.22	5.63		
PESUL1T	47.26	37.44	30.75	3.69	25.53	26.39	0.36	0.16	
MALIS2C	72.21	25.19	14.19	11.87	7.75	9.43			
INKIT3C	78.75	27.74	2.79	4.53	5.17	10.46			
ASPOR3A	132.94	22.61	0.00	11.61	0.00	40.18	0.00	0.00	0.00
ABLEG9M	46.60	35.88	32.88	6.27	27.48	54.48	21.59	4.13	
MALIS2T	39.83	44.28	62.58	25.86	17.62	10.48	19.74		
LAVPA9M	44.33	34.79	35.04	9.18	26.91				
ASPOR3C	127.73	79.06	27.86	24.53	23.50	0.00	0.00	0.00	
TOVBA9M	45.90	40.38	41.86	8.59	15.48				
PESUL3C	82.09	40.01	15.47	10.06	11.54				
LAVPA3A	83.31	41.35	25.44	10.34					
TURON3A	158.92	89.66	35.58	2.37	36.47	29.55	0.00	0.00	
ABLEG3C	89.11	76.74	8.82	0.49					
ABLEG9T	42.75	37.31	36.55	4.55	28.88	56.32	46.79	26.34	
TURON9T	62.64	47.73	86.31	76.84	10.38